



**HAL**  
open science

## Numerical Simulation: PIC models

Laurent Garrigues

► **To cite this version:**

Laurent Garrigues. Numerical Simulation: PIC models. Doctoral. First European Summer School on Electric Propulsion, Noordwijk,, France. 2023. hal-04849638

**HAL Id: hal-04849638**

**<https://hal.science/hal-04849638v1>**

Submitted on 19 Dec 2024

**HAL** is a multi-disciplinary open access archive for the deposit and dissemination of scientific research documents, whether they are published or not. The documents may come from teaching and research institutions in France or abroad, or from public or private research centers.

L'archive ouverte pluridisciplinaire **HAL**, est destinée au dépôt et à la diffusion de documents scientifiques de niveau recherche, publiés ou non, émanant des établissements d'enseignement et de recherche français ou étrangers, des laboratoires publics ou privés.

# Numerical Simulations: PIC models






**Laurent Garrigues, Senior Scientist at CNRS**



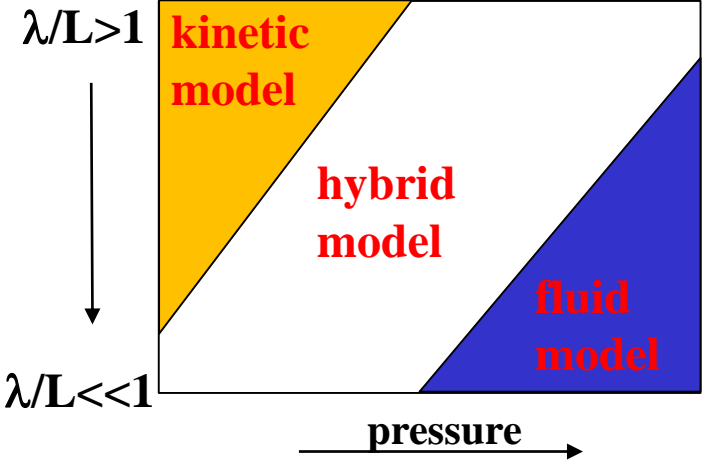
*laurent.garrigues@laplace.univ-tlse.fr*

**Laboratoire Plasma et Conversion d'Énergie – LAPLACE**  
**Université de Toulouse, CNRS-UPS-INPT**  
**31062 Toulouse Cedex 09, France**

# Outline

- **PIC algorithms** 
- **Electrostatic thrusters** 
- **Electromagnetic thrusters** 
- **Acceleration of the PIC schemes** 
- **Conclusions and perspectives** 

# Kinetic vs fluid approaches



## Boltzmann equation

$$\frac{\partial}{\partial t} f_s + \vec{v} \frac{\partial}{\partial \vec{r}} f_s + \vec{a} \frac{\partial}{\partial \vec{v}} f_s = \left\{ \frac{\partial}{\partial t} f_s \right\}_{coll}$$

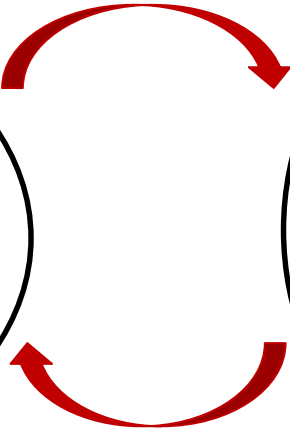
$$f_s \equiv f_s(\vec{r}, \vec{v}, t)$$

$$\vec{a} = q_s (\vec{E} + \vec{v} \times (\vec{B}_{ext} + \vec{B}_{self})) / m_s$$

## Field equations

$$[\vec{E}(\vec{r}, t), \vec{B}_{self}(\vec{r}, t)]$$

$$\rho(\vec{r}, t), \vec{J}(\vec{r}, t)$$



# Particle-In-Cell (PIC) model

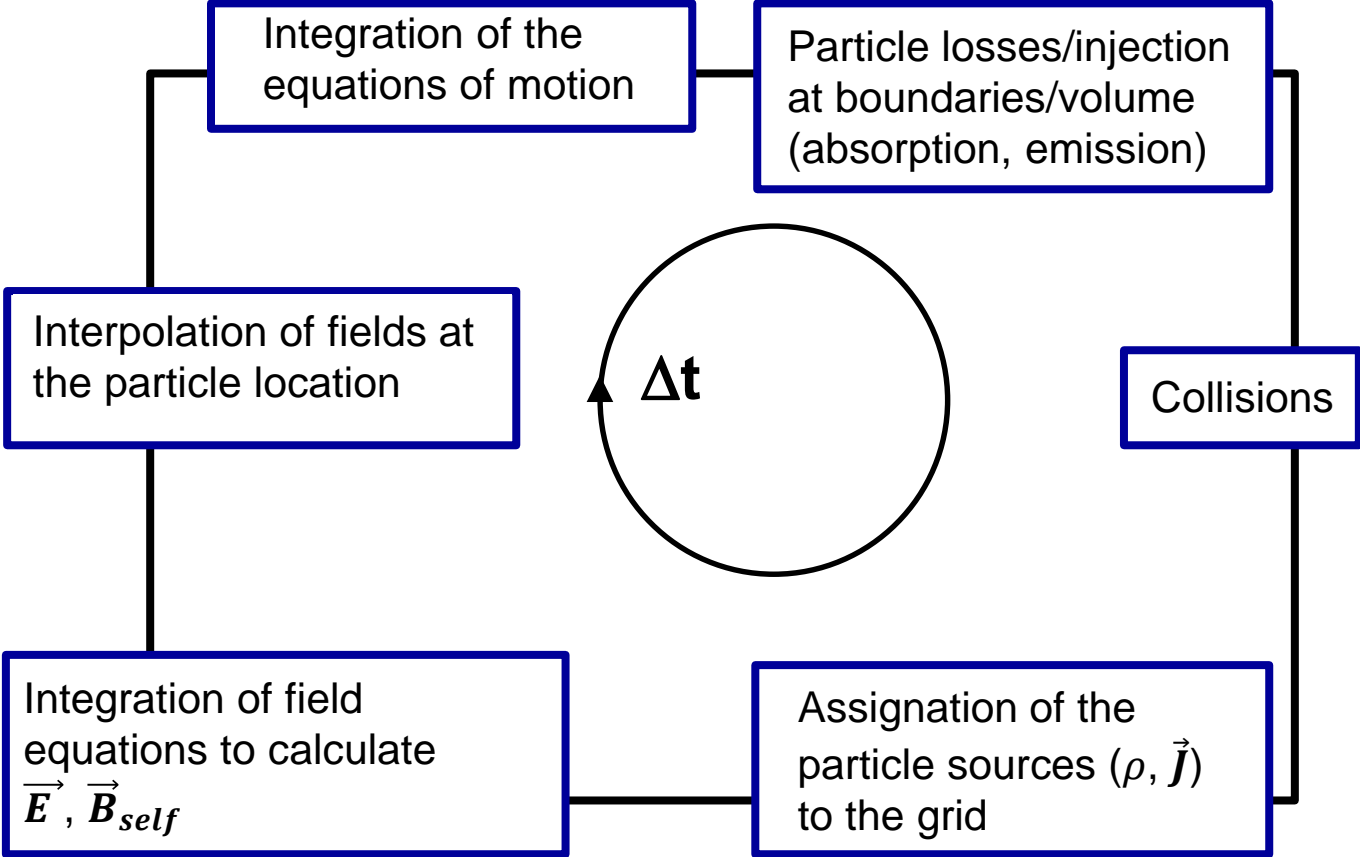
- Sampling of  $f_s$  with a finite number  $p$  of particles (**super-particules**)

$$f_s(\vec{r}, \vec{v}, t) = \sum_p f_{s,p}(\vec{r}, \vec{v}, t)$$

- Time evolution of the particles defined by position and velocity in an electric and magnetic fields generated and modified by themselves (with the potential action of an external B field), including collisions
- Introduction of a time step, a space grid mesh and a finite number of particles (and **constrains associated**)
- Self-induced B field negligible

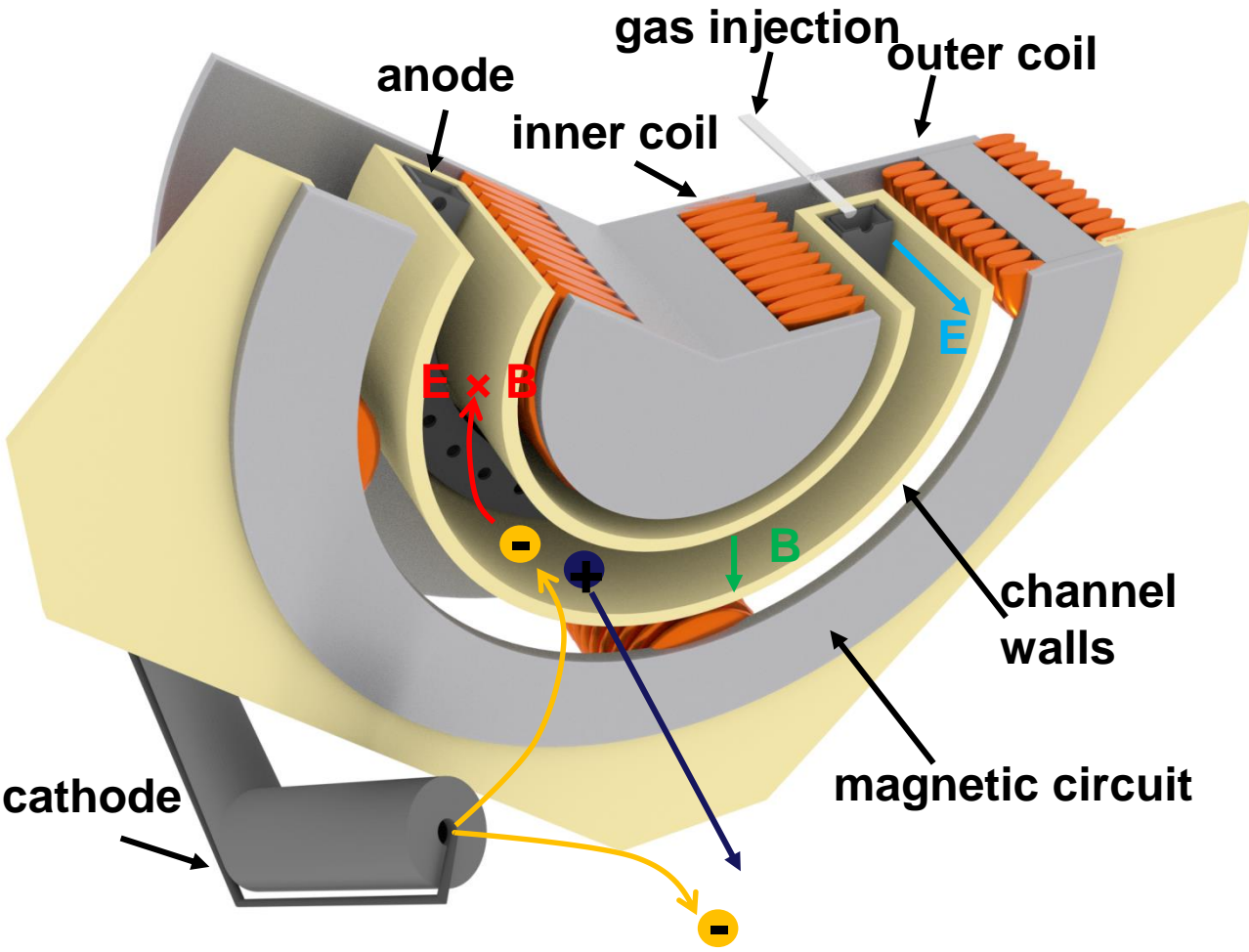
Electrostatic PIC model – ES-PIC

# PIC cycle



J. P. Verboncoeur, Plasma Phys. Control. Fusion 47, A231 (2005)

# Hall thruster



- Strongly ionization of the neutral flow
- Enhanced electron transport wo collisions?

Credit: Alexandre Guglielmi

# Hall thruster, instabilities?

- Analytical resolution – no gradients**

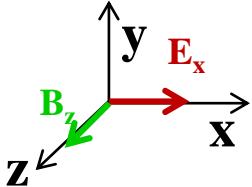
- Electrons are magnetized, Maxwellian and collisionless
- Cold ions, not magnetized and collisionless
- Coupling with Poisson’s equation
- Solution  $\phi = \phi_0 \exp[i(\vec{k} \cdot \vec{r} - \Omega t)]$
- Linearize the system of equations
- $\Omega(k)$ : dispersion relation
- Instabilities appear if  $\gamma < 0$

with  $\Omega = \overset{\text{real}}{\omega} + i\overset{\text{imaginary (growth rate)}}{\gamma}$ : frequency;  $\vec{k}$ : wave number

- Dispersion relation, electrostatic waves**

$$1 + k^2 \lambda_{De}^2 + g\left(\frac{\Omega - k_y V_E}{\omega_{ce}}, (k_x^2 + k_y^2)\rho^2, k_z^2 \rho^2\right) - \frac{k^2 \lambda_{De}^2 \omega_{pi}^2}{(\Omega - k_x V_{ib})^2} = 0$$

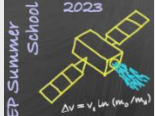
$g(\Omega, X, Y)$ : Gordeev function



$$V_E = \frac{E}{B} \quad \lambda_{De} = \sqrt{\frac{\epsilon_0 k_B T_e}{e^2 n_e}} \quad \omega_{ce} = \frac{eB}{m_e}$$

$$v_{the} = \sqrt{\frac{8k_B T_e}{\pi m_e}} \quad \rho = \frac{v_{the}}{\omega_{ce}} \quad \omega_{pi} = \sqrt{\frac{e^2 n_i}{m_i \epsilon_0}}$$

- S. P. Gary and J. J. Sanderson, *J. Plasma Physics* 4, 739 (1970)
- D. W. Forslund *et al.*, *Phys. Rev. Lett.* 25, 1266 (1970)
- M. Lampe *et al.*, *Phys. Rev. Lett.* 22, 1221 (1971)
- A. Ducrocq *et al.*, *Phys. Plasmas* 13, 102111 (2013)
- J. Cavalier *et al.*, *Phys. Plasmas* 20, 082107 (2013)





# Transition to MIA instability?

- Transition to the modified acoustic instability

- If  $\lambda_{De} < \rho$  and  $V_E < V_{the}$
- Transition to MIA
- Discrete modes

$$\omega \approx k_x V_{ib} + \frac{kc_s}{(1 + k^2 \lambda_{De}^2)^{1/2}}; \gamma \approx \sqrt{\frac{\pi m_e}{8 m_i}} \frac{k_y V_d}{(1 + k^2 \lambda_{De}^2)^{3/2}}$$

M. Lampe *et al.*, Phys. Rev. Lett. 22, 1221 (1971)

- MIA Characteristics

- Maximum growth rate
- Wave vector at maximum growth rate
- Angular frequency at maximum growth rate
- Amplitude of field oscillations
- Assuming saturation due to ion-wave trapping

$$\gamma_{max} \approx a \omega_{pi} \frac{V_E}{V_{the}}, a \sim 0.2$$

$$k_{y,max} \approx \frac{1}{\sqrt{2} \lambda_{De}}, \lambda_{y,max} \approx 2\pi \sqrt{2} \lambda_{De}$$

$$\omega_{R,max} \approx \frac{\omega_{pi}}{\sqrt{3}}$$

$$|\delta E| \approx \frac{1}{3\sqrt{2}} \frac{T_e}{\lambda_{De}}$$

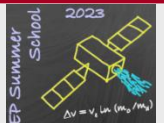
T. Lafleur *et al.*, Phys. Plasmas 23, 053503 (2016)

$$|\delta\phi| \approx \frac{1}{2} \frac{M}{e} \left( \frac{\omega_{R,max}}{k_{y,max}} \right)^2$$

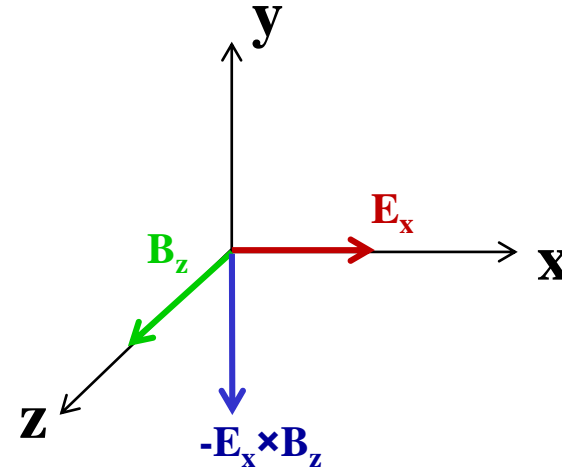
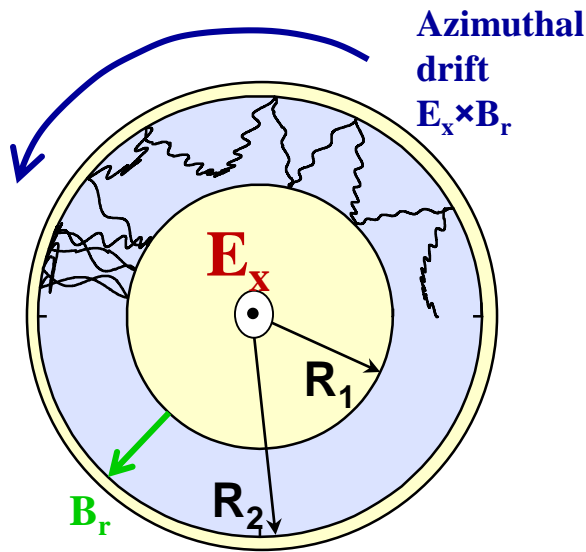
- Wavelength

$$\lambda_{y,MIA} \approx 2\pi \sqrt{2} \lambda_{De}$$

E = 200 V/cm, B = 200 G,  $n_e \sim 10^{17} \text{ m}^{-3}$ ,  $T_e \sim 50 \text{ eV}$ ,  $\lambda_{y,MIA} \sim 1 - 2 \text{ mm}$



# Hall thruster: $E \times B$ configuration

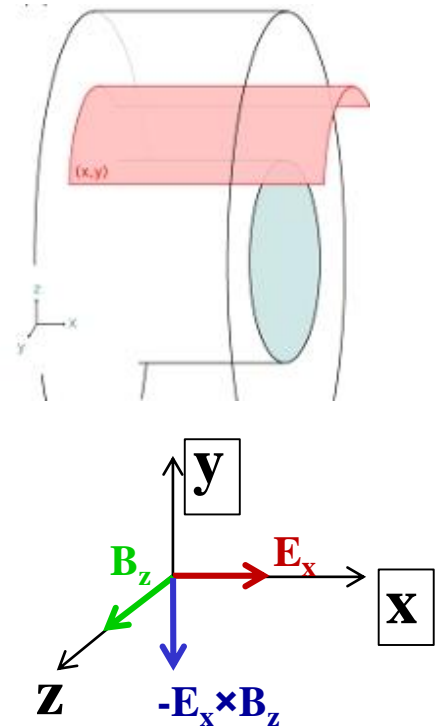
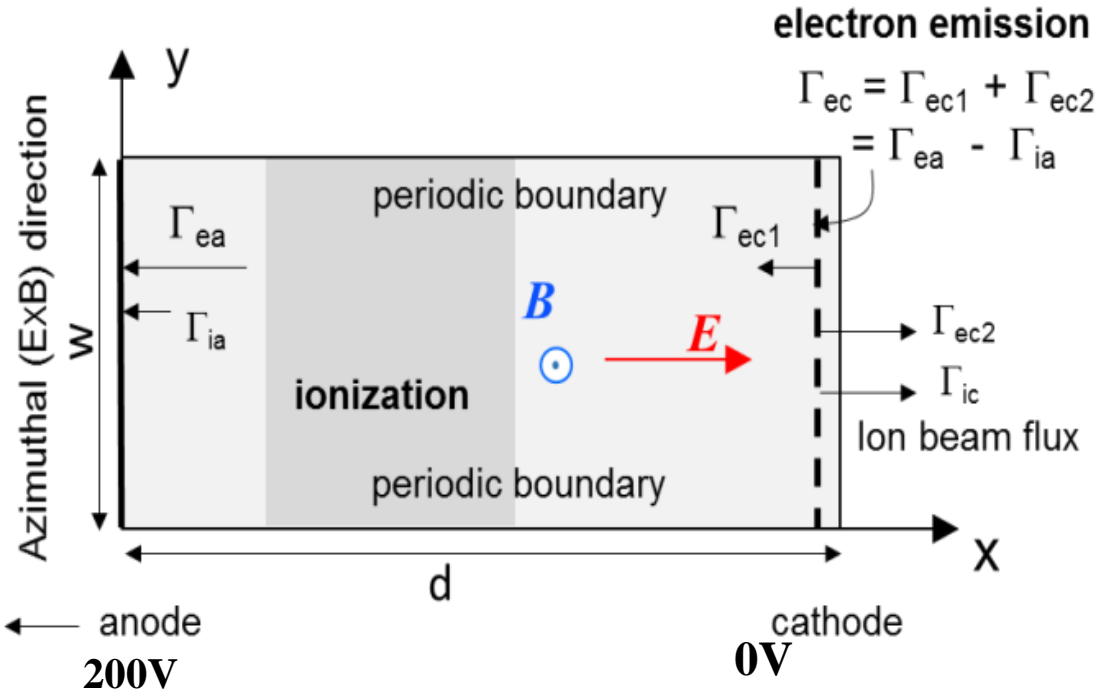


$$V_E = \frac{E \times B}{B^2} = \frac{E}{B}$$

## ■ Hall thruster characteristics

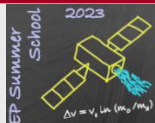
- Electrons are magnetized
- Ions are not magnetized
- Closed electron drift in the azimuthal direction
- Instabilities due to different velocity between electrons and ions in the azimuthal direction

# 2D ES-PIC simplified model – (x,y) plane (1/2)

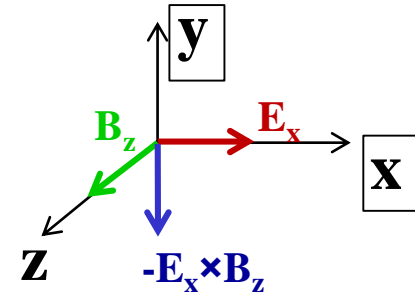
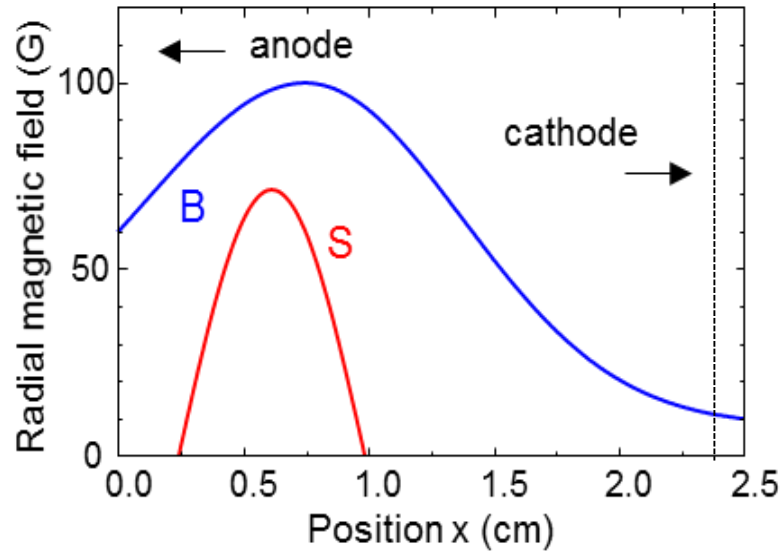


- **Explicit PIC method with OpenMP/MPI parallelization techniques**
- **Rectangular simulation domain (x,y) directions**
- **B ⊥ to simulation plane (with fixed profile)**
- **Periodic boundary conditions along y (angular sector, w = 1 cm)**
- **d= 2.5 cm, cathode @ 2.4 cm**
- **Applied voltage 200 V**

J. P. Boeuf and L. Garrigues, Phys. Plasmas 25, 061204 (2018)



# 2D PIC simplified model – (x,y) plane (2/2)



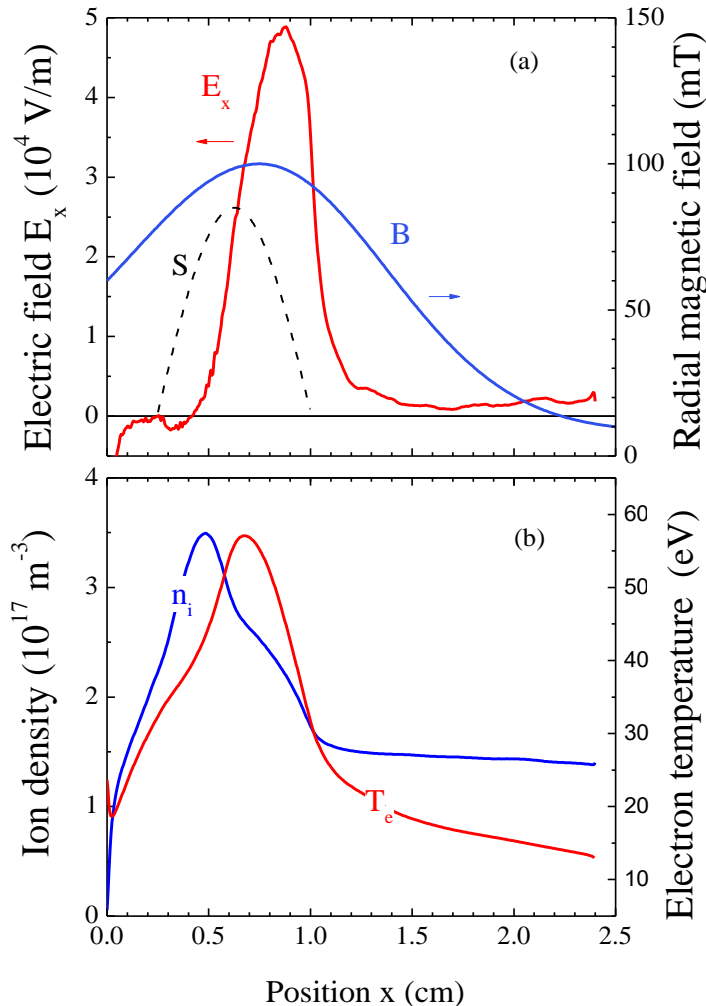
- Given source of injection of charged particles

$$J_M = e \int_0^d S(x) dx$$

- Changing  $J_M$  means changing plasma density
- No collisions

# 1D plasma properties – aver. along y and t

$$J_M = 400 \text{ A/m}^2$$



## ■ Axial electric field

- Maximum  $\sim 4 \times 10^4$  V/m
- Consistent profile with LIF measurements

S. Mazouffre *et al.*, Plasma Sources Sci. Technol. 22, 013001 (2013)

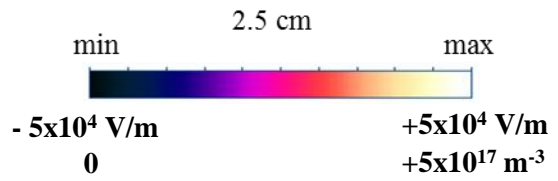
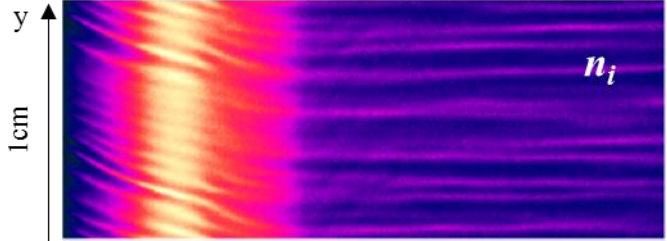
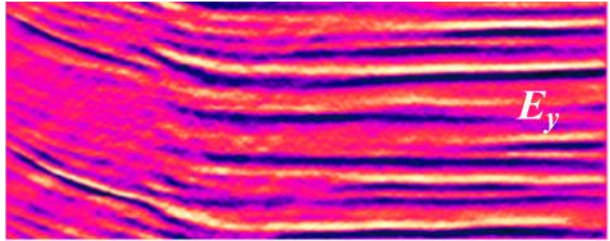
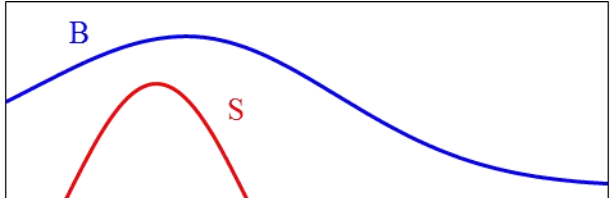
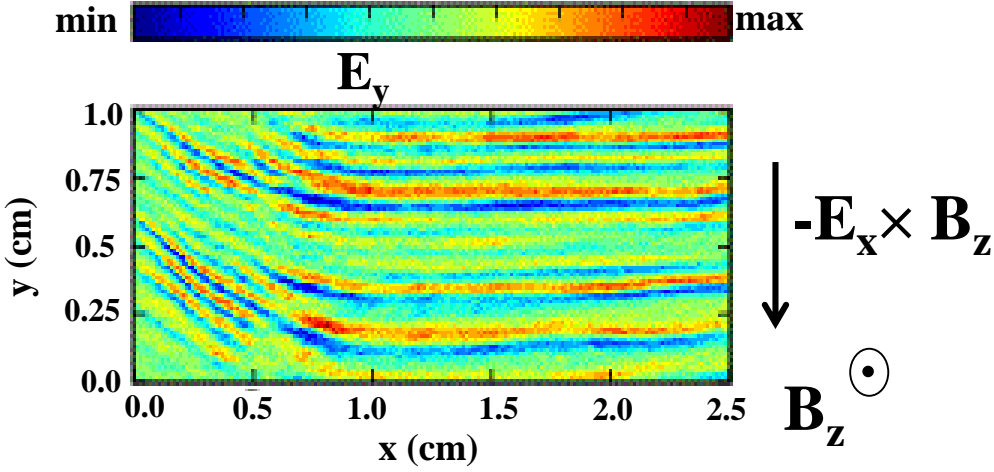
## ■ Plasma properties

- Density  $\sim 3 \times 10^{17}$  m $^{-3}$
- Electron temperature  $\sim 50$  eV consistent with Thomson scattering

T. Dubois *et al.*, IEPC, Boston, MA, 2022

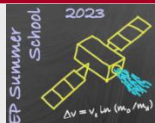
# EDI instability

$J_M = 400 \text{ A/m}^2$



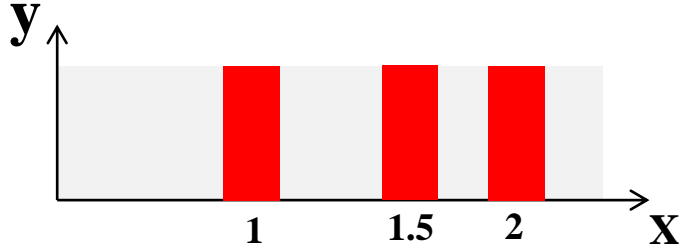
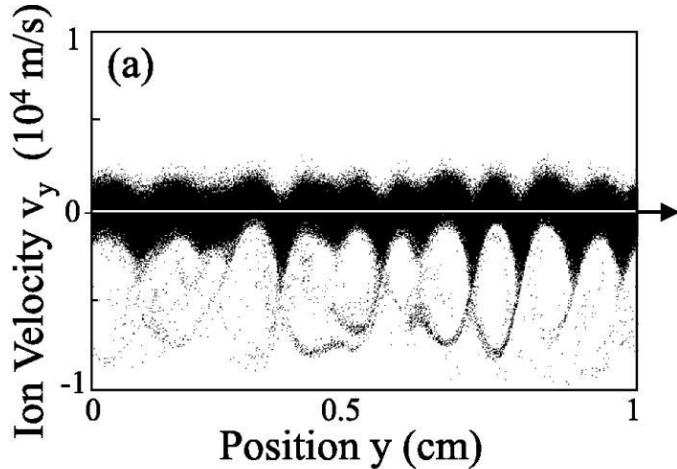
- Electron transport ensured by electron-wave interactions

J. P. Boeuf and L. Garrigues, Phys. Plasmas 25, 061204 (2018)

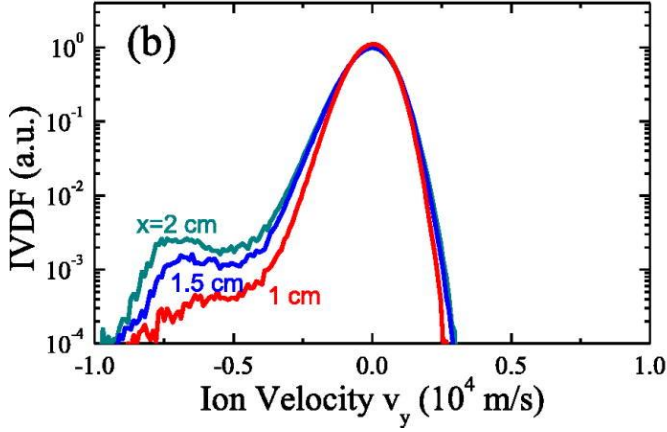


# Saturation mechanism – ion wave trapping

$J_M = 400 \text{ A/m}^2$

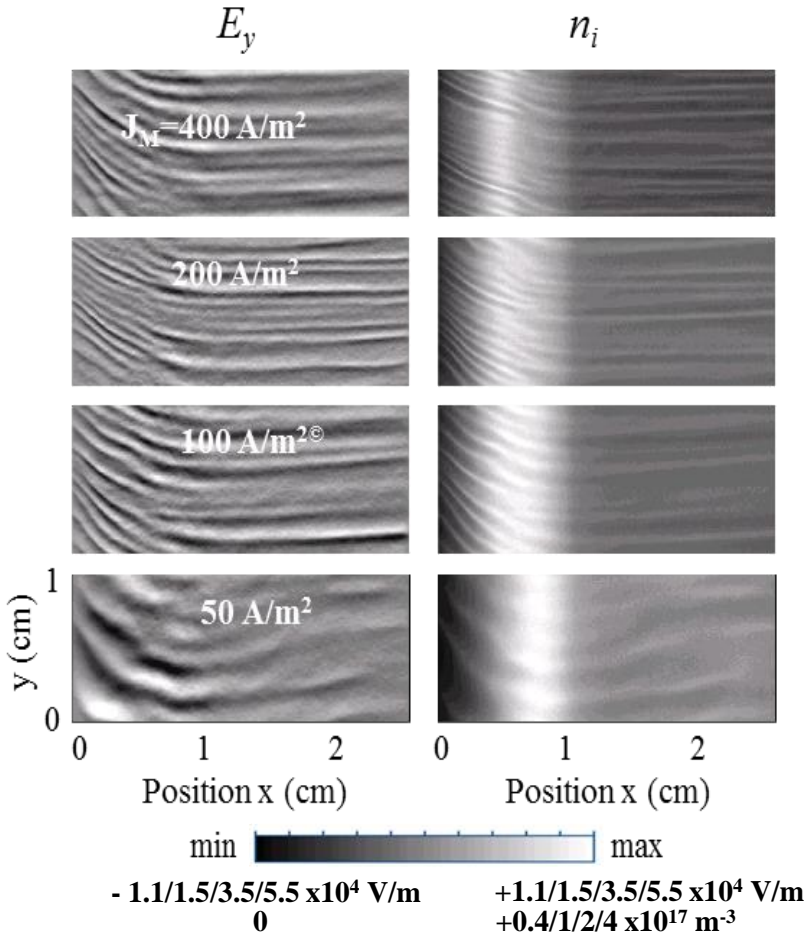


J. P. Boeuf and L. Garrigues, Phys. Plasmas 25, 061204 (2018)

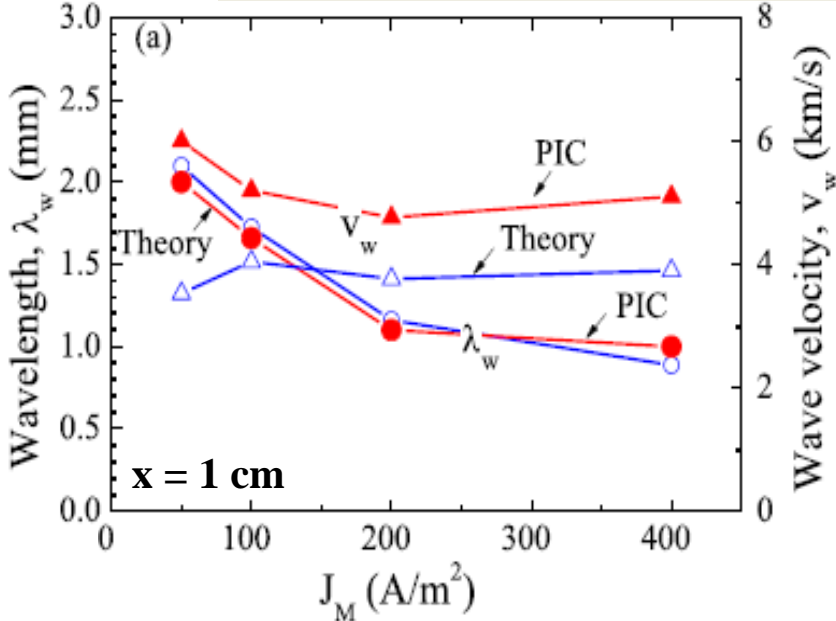


- Experimental validation from LIF measurements?

# Parametric study – plasma densities



$$k_{y,max} \approx \frac{1}{\sqrt{2}\lambda_{De}}, \lambda_{y,max} \approx 2\pi\sqrt{2}\lambda_{De}$$



$$v_w = \frac{\omega_{r,max}}{k_{y,max}} = c_s \sqrt{\frac{2}{3}}$$

J. P. Boeuf and L. Garrigues, Phys. Plasmas 25, 061204 (2018)



# How the instability affects the transport (1/2)?

T. Lafleur *et al.*, Plasma Sources Sci. Technol. 27, 015003 (2018)

## ■ Fluid momentum equation

“e-i friction”

$$\frac{d}{dt}(m_e n_e \mathbf{v}_e) + \nabla \cdot (m_e n_e \mathbf{v}_e \mathbf{v}_e) = e n_e (\mathbf{E} + \mathbf{v}_e \times \mathbf{B}) - \nabla \cdot (\mathbf{\Pi}_e) + \mathbf{R}_{en} + \mathbf{R}_{ei}$$

## ■ Calculations of moments from PIC simulations

$$n_e = \int_{-\infty}^{\infty} f_e(\mathbf{w}) d^3 w$$

$$\mathbf{R}_{en} = -m_e n_g \int_{-\infty}^{\infty} \sigma_{en}(w) w \mathbf{w} f_e(\mathbf{w}) d^3 w$$

$$n_e \mathbf{v}_e = \int_{-\infty}^{\infty} \mathbf{w} f_e(\mathbf{w}) d^3 w$$

$$\mathbf{R}_{ei} = e \langle \delta n_e \delta \mathbf{E} \rangle = e \langle [\langle n_e \rangle_t - n_e(t)] [\langle \mathbf{E} \rangle_t - \mathbf{E}(t)] \rangle_t$$

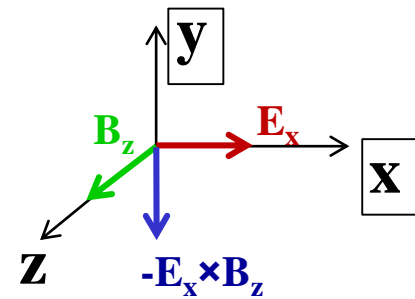
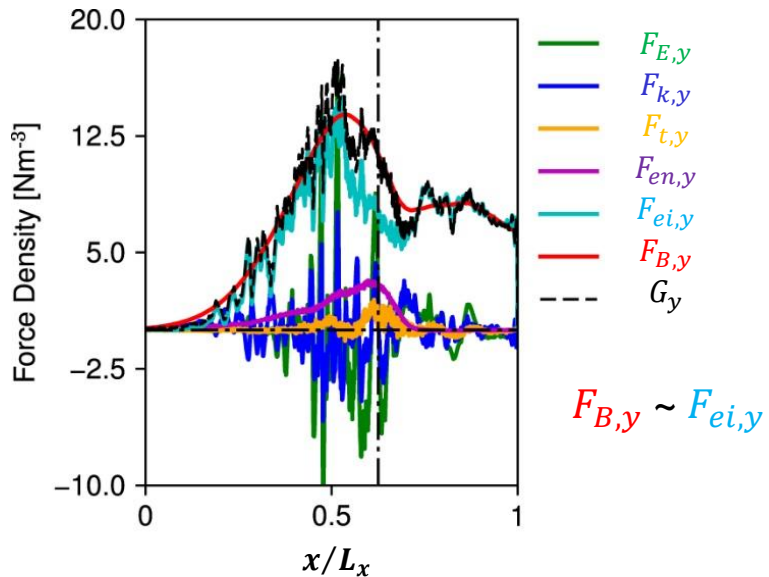
$$\mathbf{\Pi}_e = m_e \int_{-\infty}^{\infty} (\mathbf{w} - \mathbf{v}_e)(\mathbf{w} - \mathbf{v}_e) f_e(\mathbf{w}) d^3 w$$

# How the instability affects the transport (1/2)?

- Projection along the  $y$  – azimuthal direction

$$\left\langle \frac{d}{dt} (m_e n_e v_{e,y}) + \frac{d}{dx} (m_e n_e v_{e,x} v_{e,y}) \right\rangle_y = \left\langle en_e (E_y + v_{e,x} B_z) - \frac{d\Pi_{e,xy}}{dx} + R_{en,y} + R_{ei,y} \right\rangle_y$$

$$\underbrace{-en_e v_{e,x} B_z}_{F_{B,y}} = \underbrace{\frac{d}{dt} (m_e n_e v_{e,y})}_{F_{t,y}} + \underbrace{\frac{d}{dx} (m_e n_e v_{e,x} v_{e,y})}_{F_{k,y}} + \underbrace{\frac{d\Pi_{e,xy}}{dx}}_{G_y} - \underbrace{en_e E_y}_{F_{E,y}} - \underbrace{R_{en,y}}_{F_{en,y}} + \underbrace{R_{ei,y}}_{F_{ei,y}}$$



T. Lafleur *et al.*, Plasma Sources Sci. Technol. 27, 015003 (2018)

## LANDMARK

Low temperature magnetized plasma benchmarks

- HOME
- PHYSICS ISSUES
- TEST CASES
- WORKSHOP
- FORUM
- MEMBERS
- CONTACT

### Test Cases

Three first test cases have been defined and are described below. These cases correspond to typical conditions of Hall thrusters. The problem has however been oversimplified in order to address specific issues related to the numerical method and/or to physics questions. Other test cases will be proposed in the future

#### Test Case 1 - 1D azimuthal PIC simulation of the ExB EDI

This test case is aimed at studying the possible development of microinstabilities induced by the large ExB electron drift in the magnetic barrier of a Hall thruster. The Electron Cyclotron Drift Instability (which we call ExB Drift Instability, ExB EDI, in the present context) studied in the 1970's in space plasmas, has been evidenced in axial-azimuthal PIC simulations of Hall thrusters. The proposed benchmark is aimed at studying the ExB EDI under 1D conditions (constant E and B, and description of the ExB, azimuthal direction) and the conditions of the possible transition to an ion acoustic instability. The effects of numerical noise, accuracy of the simulations, and spatial periodicity in the ExB direction must also be evaluated

details

#### Test Case 2a - 2D axial-azimuthal PIC simulation of the ExB EDI

Here we study the ExB EDI under slightly more realistic conditions that can naturally take into account the finite transit time of electrons in the acceleration region, and the effects of density and magnetic field gradients. We simplify the problem by assuming a given ionization rate profile. This suppresses the non-linear coupling of the plasma density and atom density leading to the well known low frequency ("breathing") oscillations of Hall thrusters. The proposed benchmark allows to study the formation, convection and saturation of the ExB EDI. The issues are the transition to an ion acoustic instability, the effect of the instability on the anomalous electron cross-field mobility, the possible effect of numerical noise and of the finite period of the model in the azimuthal direction.

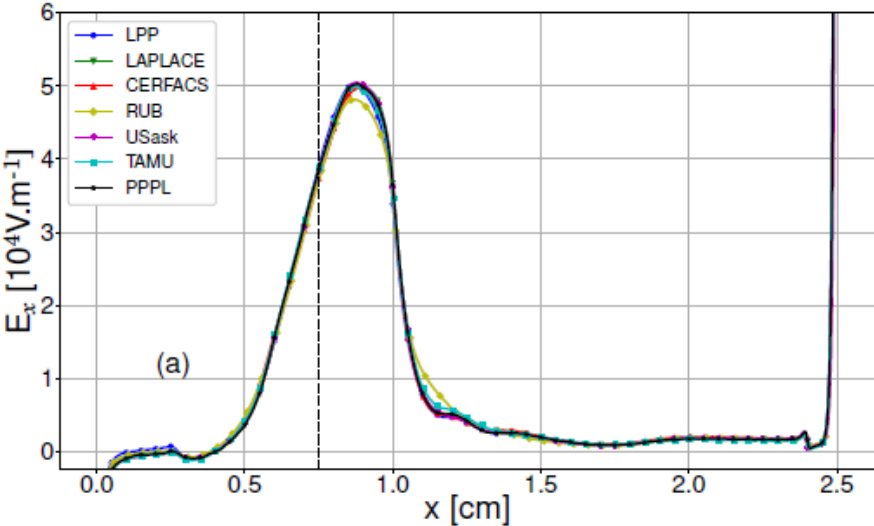
details

#### Test Case 2b - 2D radial-azimuthal PIC simulation of the ExB EDI

In this case the ExB EDI is studied in the radial and azimuthal directions. The electron and ion transport in the axial direction is described as in Test Case 1 (constant electric field in the axial direction, constant magnetic field in the radial direction).

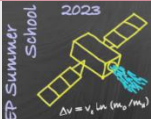
details

### Test Case 2a results



T. Charoy *et al.*, Plasma Sources Sci. Technol. 28, 105010 (2019)

W. Villafana *et al.*, Plasma Sources Sci. Technol. 30, 075002 (2021)



# Numerical models – Test Case 2a

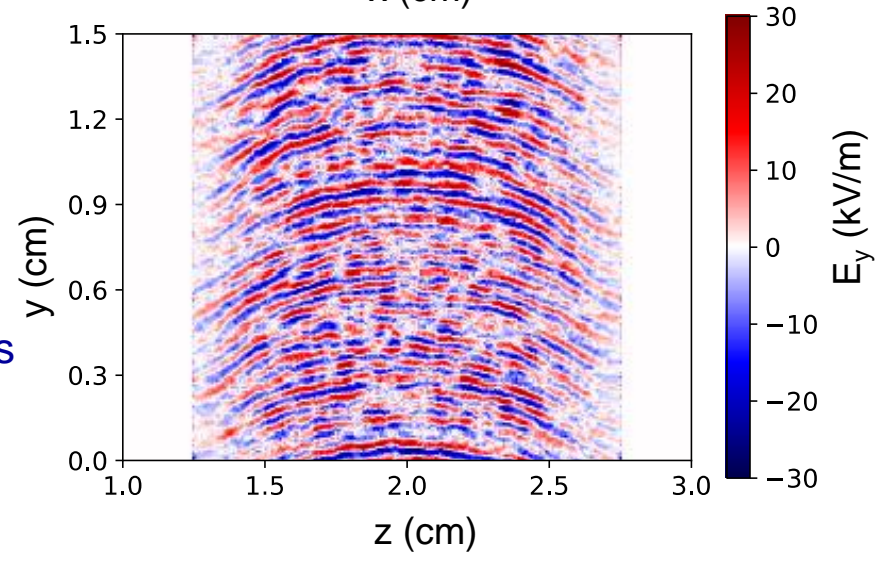
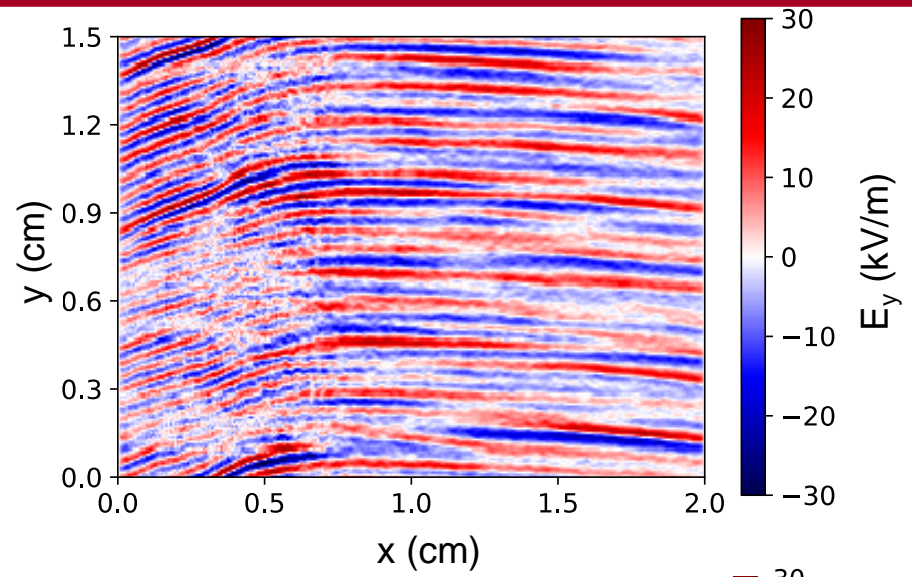
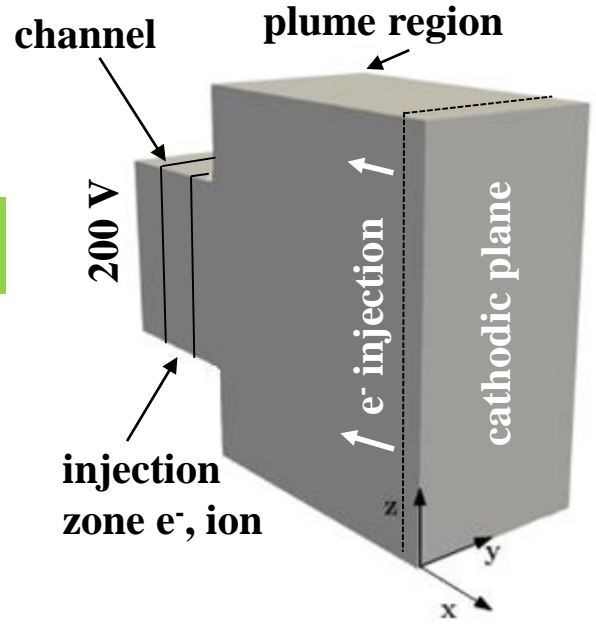
Table 2: Main codes specificities.

	LPP	LAPLACE	CERFACS	RUB	USask	TAMU	PPPL
<b>Algorithms</b>							
<b>Pusher solver</b>	Explicit	Explicit	Explicit	Implicit	Explicit	Explicit	Explicit
<b>Poisson solver</b>	Hypre	Pardiso	Maphys	FFT Thomas	FFT	Hypre	Hypre
<b>Floating-point precision</b>	Double	Single(pusher) Double (Poisson)	Double	Single(pusher) Double (Poisson)	Double	Double	Double
<b>Code acceleration</b>							
<b>Architecture</b>	CPU	CPU	CPU	GPU	CPU	CPU	CPU
<b>Parallelization</b>	MPI	MPI/OpenMP	MPI	CUDA	MPI	MPI	MPI/OpenMP
<b>Decomposition</b>	Domain	Particle	Domain	Both	Domain	Particle	Particle
<b>Language</b>	Fortran	Fortran	Fortran	C+Cuda C	Fortran	C++	C
<b>Simulation times (days)</b>							
<b>Case 1</b> ( $N_{ppc,ini} = 150$ )	8 (360 CPU)	5 (108 CPU)	7 (360 CPU)	14 (1 GPU)	21 (32 CPU)	15 (300 CPU)	2.5 (224 CPU)
<b>Case 2</b> ( $N_{ppc,ini} = 75$ )	5 (360 CPU)	3 (108 CPU)	4 (360 CPU)	9 (1 GPU)	11 (32 CPU)	11 (200 CPU)	2.5 (112 CPU)
<b>Case 3</b> ( $N_{ppc,ini} = 300$ )	14 (360 CPU)	6 (180 CPU)	13 (360 CPU)	14 (2 GPU)	20 (64 CPU)	22 (400 CPU)	2.5 (448 CPU)

T. Charoy *et al.* , Plasma Sources Sci. Technol 28, 105010 (2019)

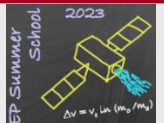
# 3D PIC simplified model (1/2)

G. Fubiani *et al.*  
ICPIG (2023)

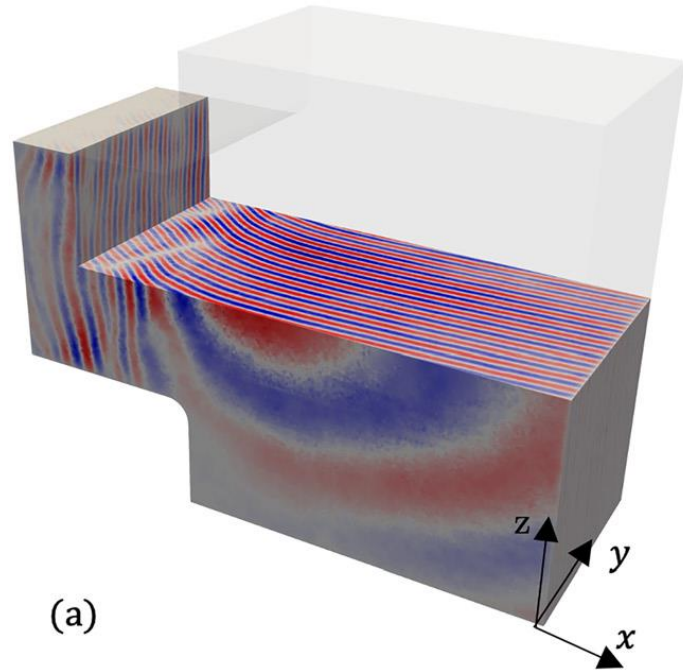
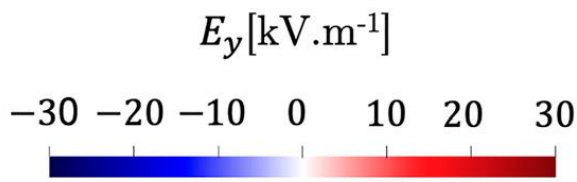
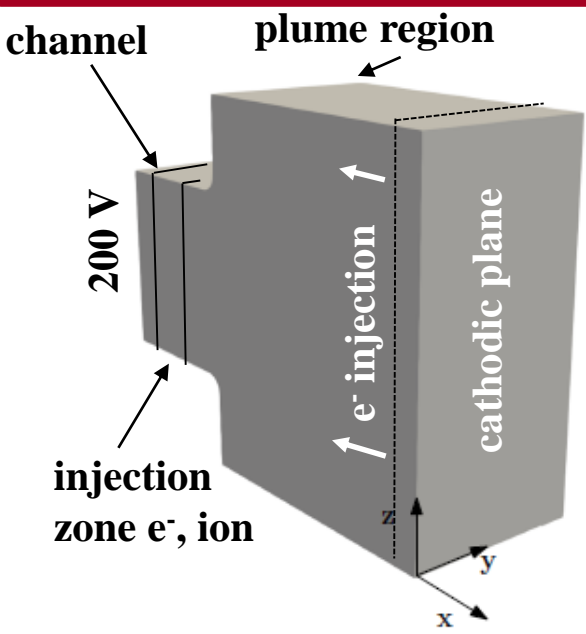


- $E_y$  fluctuating field divided by 2-3
- Compared to 2D simulations more closer to Thomson scattering measurements

S. Tsikata *et al.*, Phys. Plasmas 17, 112110 (2010)



# 3D PIC simplified model (2/2)



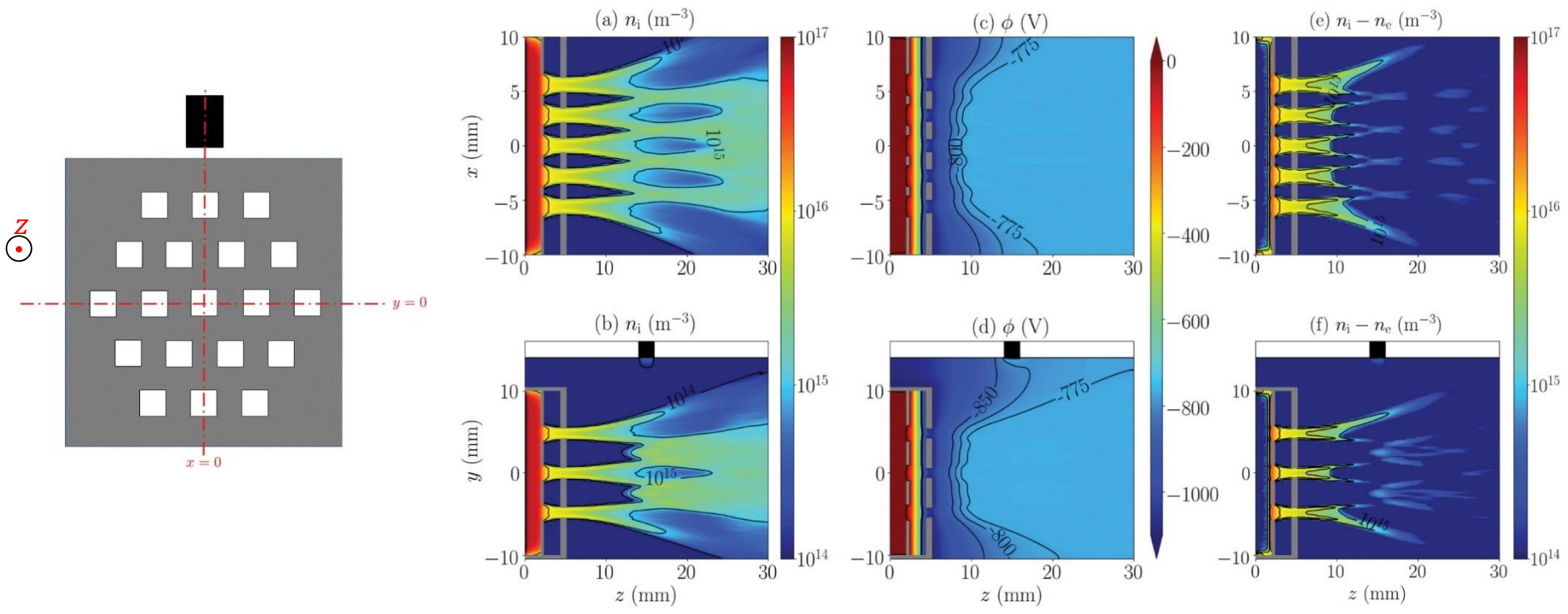
W. Villafana *et al.*,  
Phys. Plasmas  
30, 033503 (2023)

- AVIP-PIC code developed @ CERFACS, Toulouse, France (tetrahedra)
- Very long time consuming – 1-2 months on 3000 cores (1Mhrs)
- Very close results than standard 3D Cartesian PIC approach

# Gridded ion engine (GIE)



- 3D hybrid model – electron-fluid and ion-PIC
- Beamlet extraction



J. Perales-Diaz *et al.*, Plasma Sources Sci. Technol 30, 105023 (2021)

# Inductively coupled plasma thrusters

- Plasma coupling with the antenna - GIE - RIT

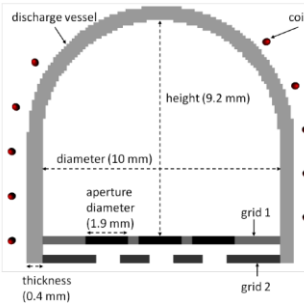
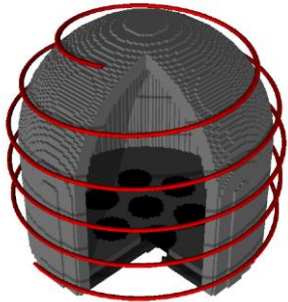
$$\left(\Delta - \mu_0 \varepsilon_0 \frac{\partial^2}{\partial t^2}\right) \mathbf{E}(\mathbf{r}, t) = \mu_0 \frac{\partial}{\partial t} \mathbf{j}(\mathbf{r}, t)$$

- Harmonic expansion – azimuthal component

$$(\Delta + \mu_0 \varepsilon_0 \omega^2) \tilde{E}_\theta = i\omega \mu_0 \tilde{j}_\theta = i\omega \mu_0 [\tilde{j}_{\theta, \text{coil}} + \tilde{j}_{\theta, \text{electron}}]$$

R. Henrich *et al.*, IEPC (2017)

- 3D parallelized EM-PIC applied to the  $\mu\text{N-RIT}$  operation



100<sup>3</sup> cells

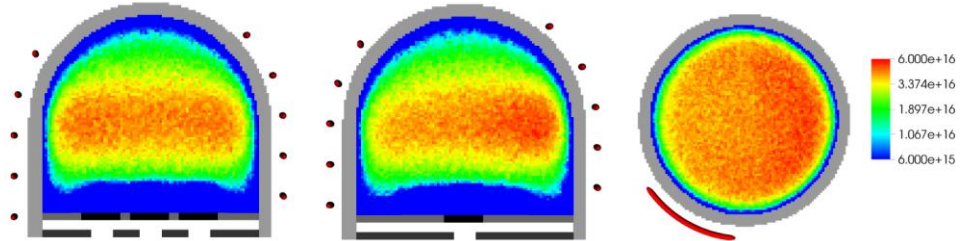


Figure 3: Electron density in 1/m<sup>3</sup> for a  $\mu\text{N-RIT}$  1.0: x-z plane (left), y-z plane (middle) and x-y plane at position 4 mm above grid 1 (right)

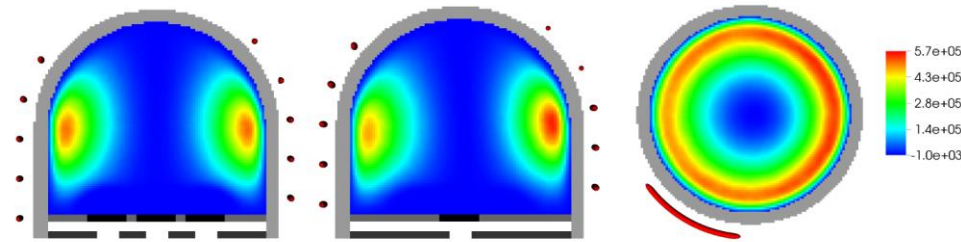


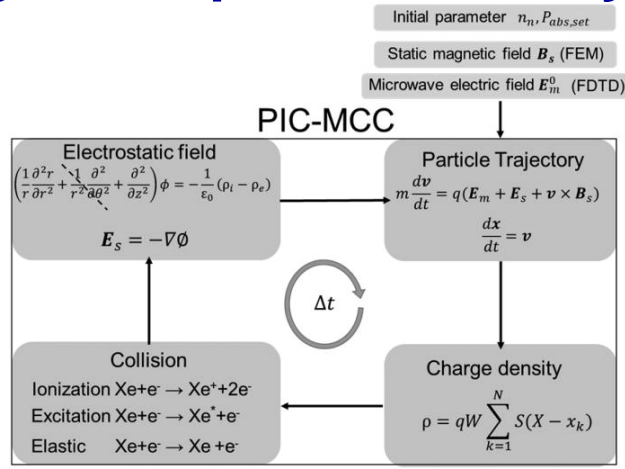
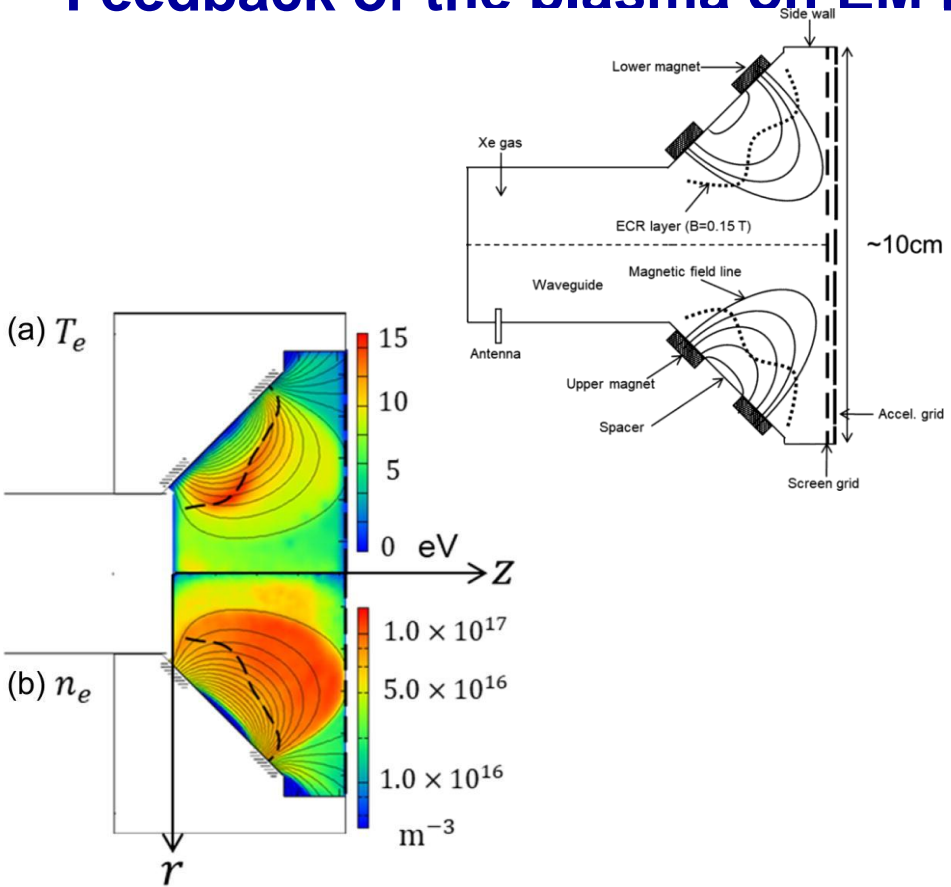
Figure 8: Power deposition in W/m<sup>3</sup> for a  $\mu\text{N-RIT}$  1.0: x-z plane (left), y-z plane (middle) and x-y plane at position 4 mm above grid 1 (right)



# $\mu\text{W}$ driven ECR plasma thrusters



- Magnetostatic field +  $\mu\text{W}$  to enhance electron heating
- Feedback of the plasma on EM ignore if plasma density  $< n_c$

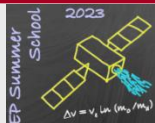


## $\mu\text{ECR-GIE}$

Y. Yamashita *et al.*,  
 Phys. Plasmas  
 26, 073510 (2019)

- Coupling waves and plasma, 1D

J. Porto *et al.*, Phys. Plasmas 30, 023506 (2023)



# Methods to overcome explicit constraints

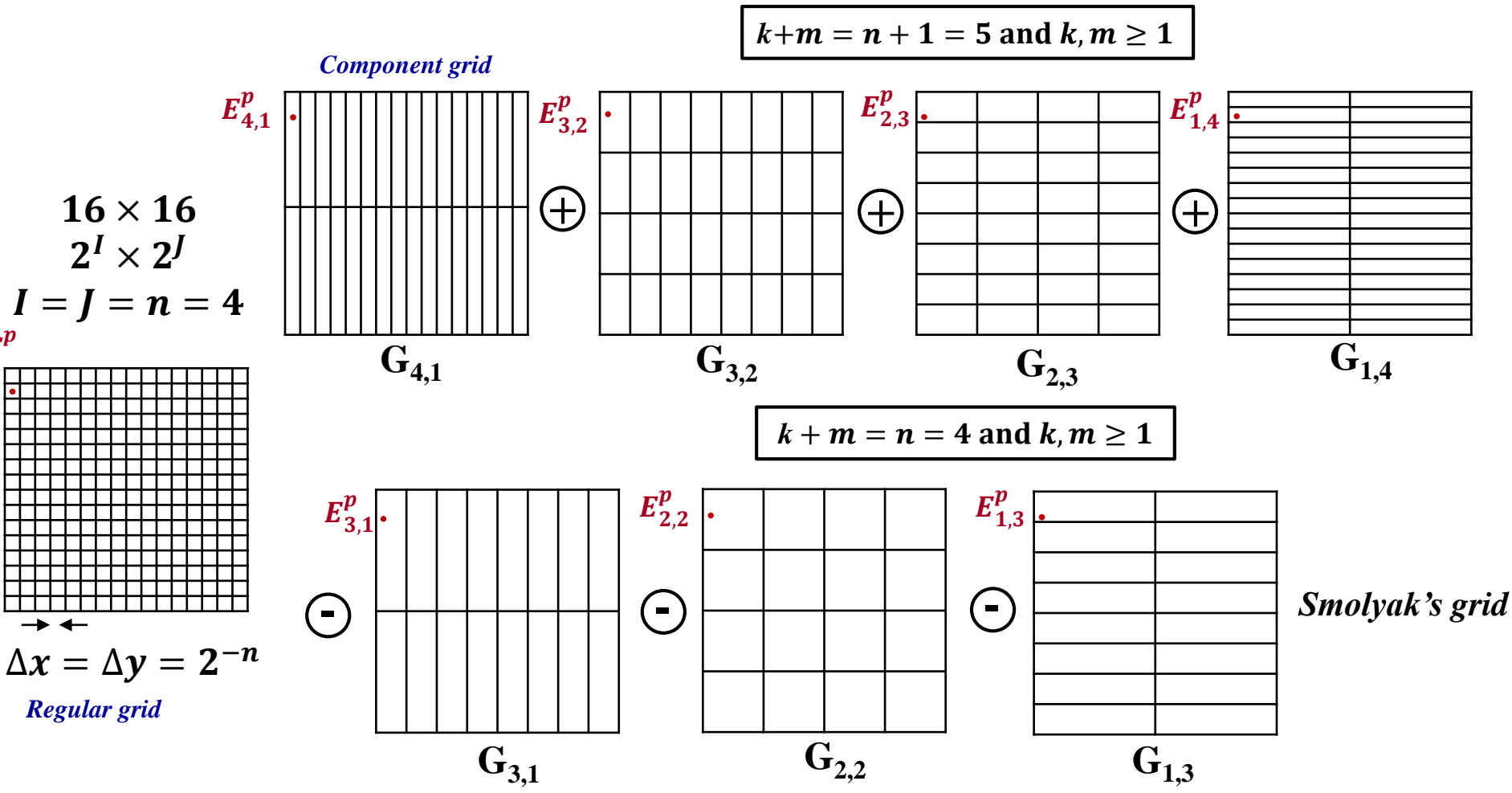
- Easy to implement but constrains on
  - Time step (plasma frequency) and grid spacing (Debye length)
  - High computational time: large density and/or large dimensions
  - Coupling with EM waves: FDTD scheme needs with CFL condition with  $c$  (light velocity)
- High Performance Computing techniques
- Overcome time step and grid mesh size constraints?
  - “scaling” method, reduced plasma density G. Fubiani *et al.*, New J. Phys. 19, 015002 (2017)
  - Fully implicit method G. Chen *et al.*, J. Comput. Phys. 230, 7018 (2011)
  - Energy conserving scheme (ECSIM) G. Lapenta, J. Comput. Phys. 334, 349 (2017)
- Reduce statistical error – numerical noise?

**Use of a sparse grid approach**

# Sparse grid methods

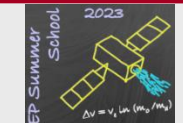
- Classical discretization on uniform Cartesian grid meshes: the total number of unknowns is proportional to  $M^d$  ( $M$  degree of freedom in each direction,  $d$  dimensionality of the problem)
- Sparse grid methods: reduction of the complexity of discrete problem by breaking the exponential increase of the number of degrees of freedom with respect to the dimensionality of the problem
- Sparse grid techniques
  - Define a hierarchy of anisotropic grids with a coarser resolution
  - Reconstruction of the solution on the initial Cartesian grid using combination techniques
  - Preserving second order approximation (for  $d > 1$ )
- Examples
  - Resolution of Navier-Stokes equation **A. Rütgers and M. Griebel, Applied Math. and Comp. 319, 425 (2018)**
  - Quantum mechanics: Schrödinger equation **J. Garcke and M. Griebel, JCP 165, 694 (2000)**
  - Plasma physics: gyrokinetic Vlasov equation **D. Pflüger et al., Euro-Par 2014: Parallel Processing (2014)**
  - Financial mathematics: Black-Scholes equation **H. J. Bungartz et al., J. Comput. Applied Math. 236, 3741 (2012)**

# Construction of sparse grid domains

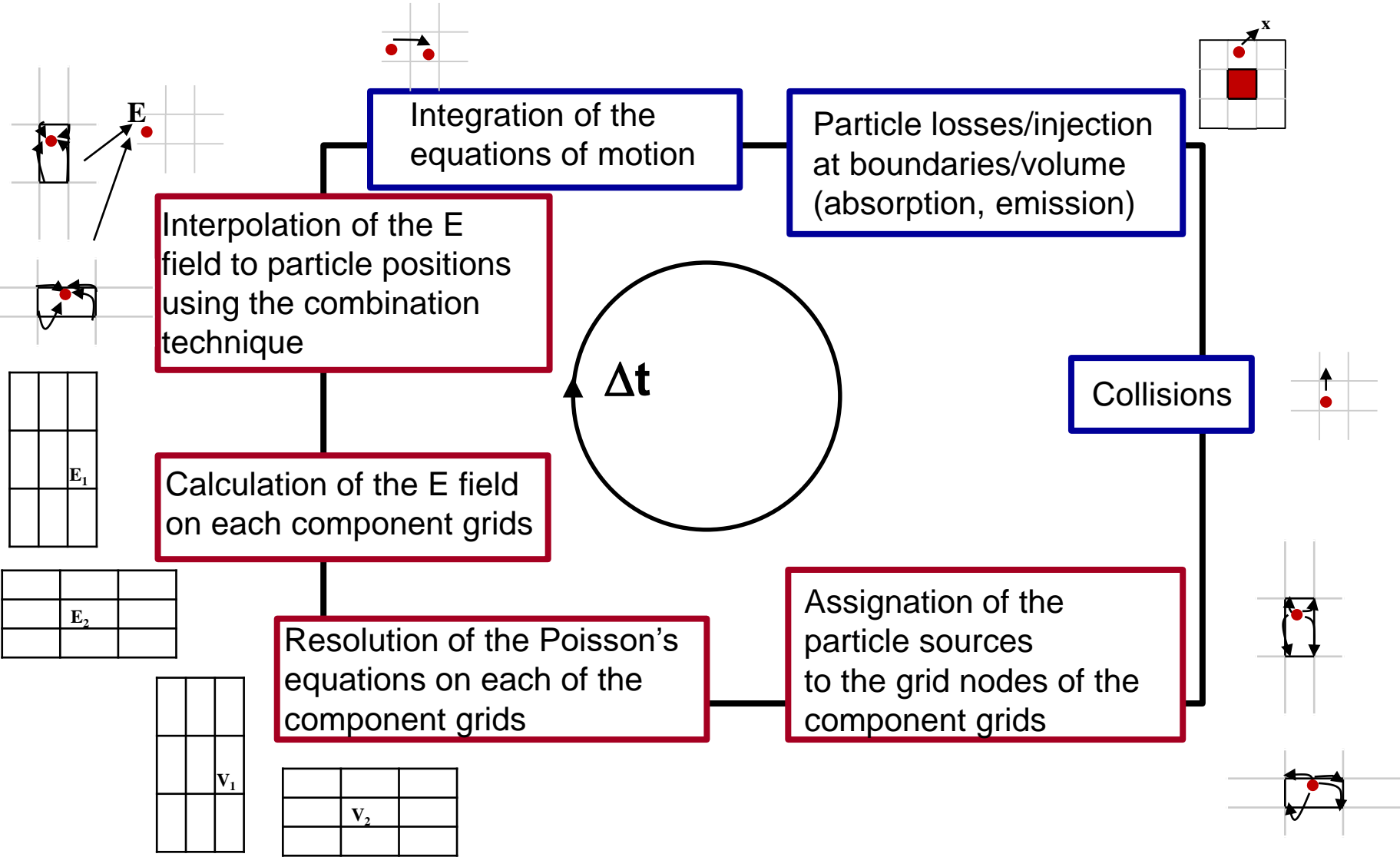


## Combination technique

$$E^p \cong \sum_{k+m=n+1} E_{k,m}^p - \sum_{k+m=n} E_{k,m}^p$$



# ES-PIC cycle revisited with sparse approach

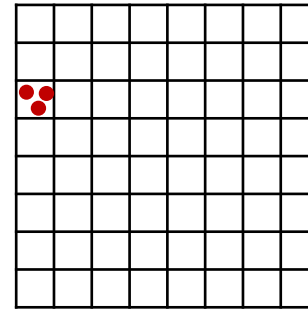


# Error: Sparse vs Std PIC approaches (1/2)

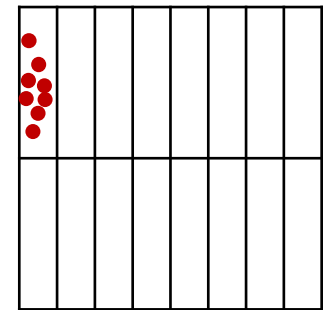
## Numerical noise

Reduction with sparse grids thanks to large volume

Error associated  $\varepsilon_s = \underbrace{|\log h_n|^{d-1}}_{\text{sparse}} \left(\frac{1}{Nh_n}\right)^{1/2} \leq \underbrace{\left(\frac{1}{Nh_n^d}\right)^{1/2}}_{\text{standard}}$

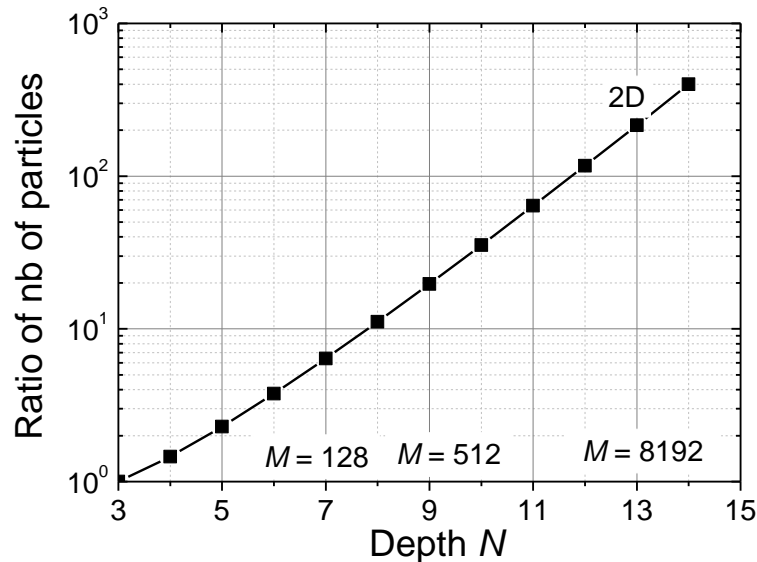


Regular grid  
 $h_n$



Component grid

**Much less particles with sparse approach for same statistical error**



ESAIM: M2AN 56 (2022) 1809–1841

<https://doi.org/10.1051/m2an/2022055>

SPARSE GRID RECONSTRUCTIONS FOR PARTICLE-IN-CELL METHODS

FABRICE DELUZET<sup>1,2</sup>, GWENAELE FUBIANI<sup>3</sup>, LAURENT GARRIGUES<sup>3</sup>,  
CLÉMENT GUILLET<sup>1,2,3,\*</sup> AND JACEK NARSKI<sup>3</sup>

# Error: Sparse vs Std ES-PIC approaches (2/2)

ESAIM: M2AN 56 (2022) 1809–1841

<https://doi.org/10.1051/m2an/2022055>

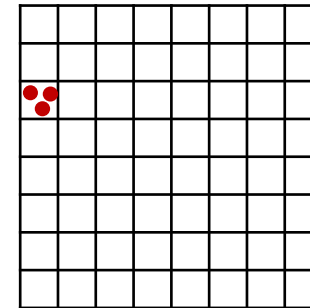
SPARSE GRID RECONSTRUCTIONS FOR PARTICLE-IN-CELL METHODS

FABRICE DELUZET<sup>1,2</sup>, GWENAEL FUBIANI<sup>3</sup>, LAURENT GARRIGUES<sup>3</sup>,  
CLÉMENT GUILLET<sup>1,2,3,\*</sup> AND JACEK NARSKI<sup>3</sup>

## ■ Grid-based error

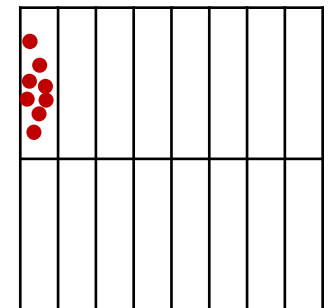
- A slight increase with sparse grids

- Error associated  $\varepsilon_s = \underbrace{|\log h_n|^{d-1}}_{\text{sparse}} h_n^d \geq \underbrace{h_n^d}_{\text{standard}}$



Regular grid

$h_n$



Component grid

- Momentum and total charged are conserved, not energy (as explicit standard ES-PIC)

## ■ Others benefits for sparse grid PIC algorithms

- Gain in memory footprint with less total number of particles
- Saving time in the resolution of Poisson's equation

# First plasma simulations

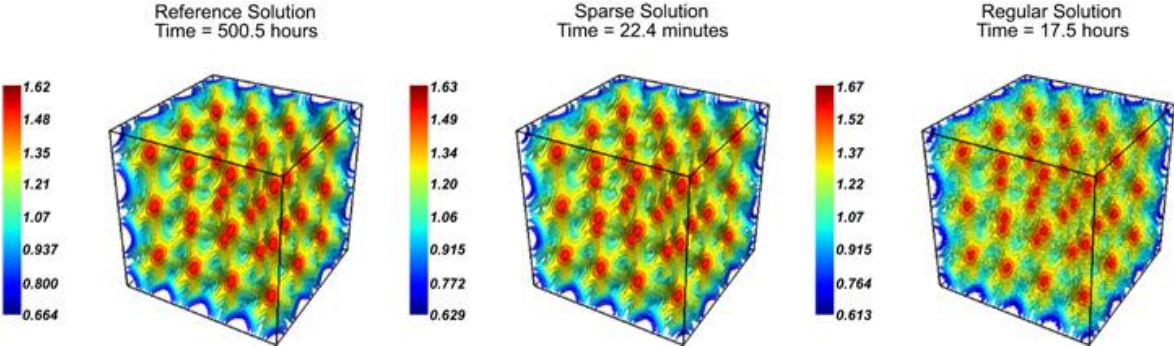
- **Applicability to ES-PIC techniques**

- Ions at rest
- Periodic boundary conditions
- No collisions

L. F. Ricketson and A. J. Cerfon, PPCF 59, 024002 (2017)

- **Numerical tests**

- Linear/non linear Landau damping
- Diocotron instability



■ **Extension to low temperature plasmas?**

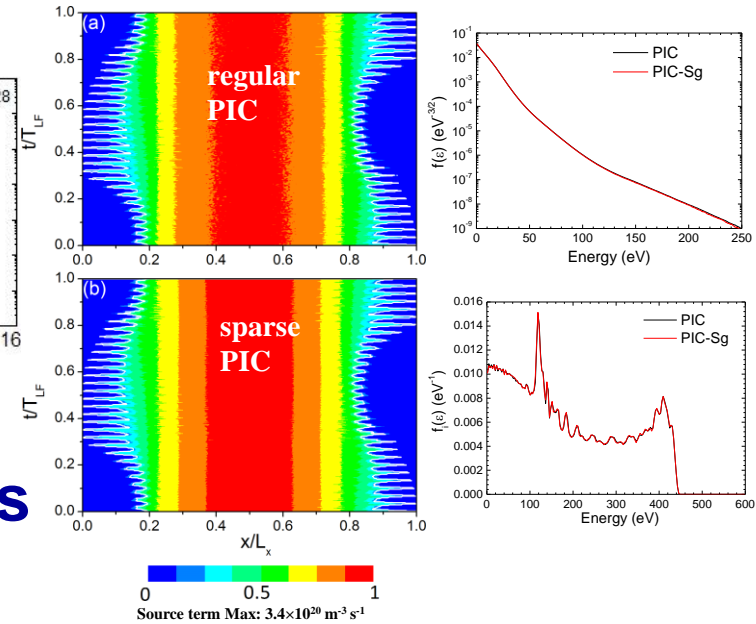
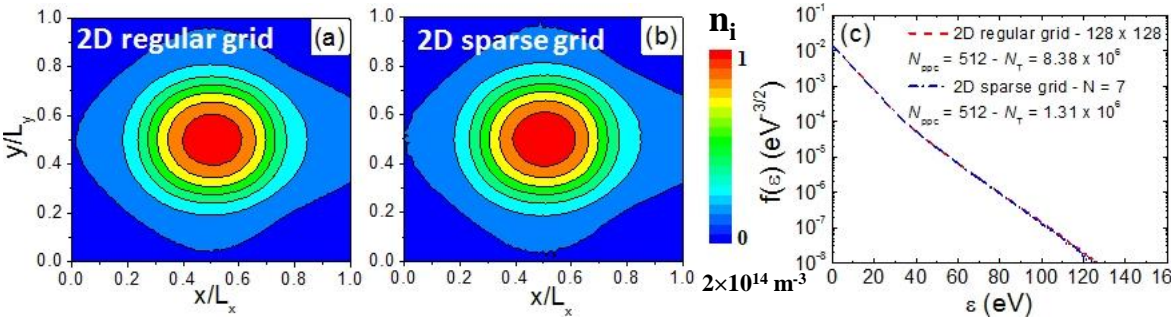
3D non linear Landau damping  
Comparison of density reference solution computed ( $128 \times 128 \times 128$ ) using regular PIC (left),  $\sim 30$  simulations, sparse solution on grid with  $N_{pc} = 800$  (center), and regular-PIC solution on grid with  $N_{pc} = 800$  (right)



# RF capacitive discharges

- Self-consistent description of the discharge
- Motion of ions
- Time and space evolution of sheaths
- Collisions between electrons/ions and neutrals
- Single-frequency RF capacitive discharges

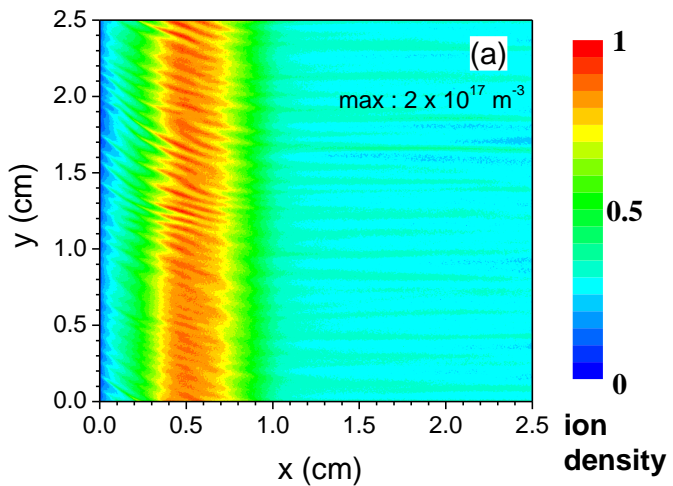
L. Garrigues *et al.*,  
J. Appl. Phys. 129, 153303 (2021)



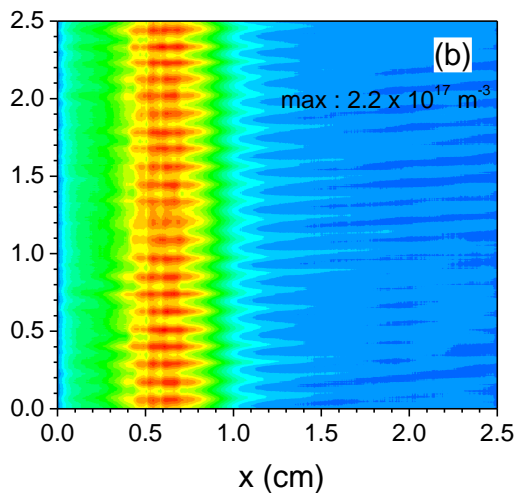
- Dual-freq. RF capacitive discharges

L. Garrigues *et al.*, ICPIG (2023)

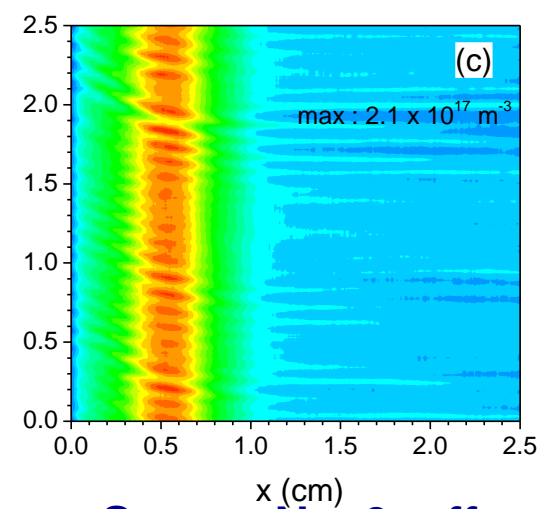
# HT - 2D benchmark, axial-azimuthal directions



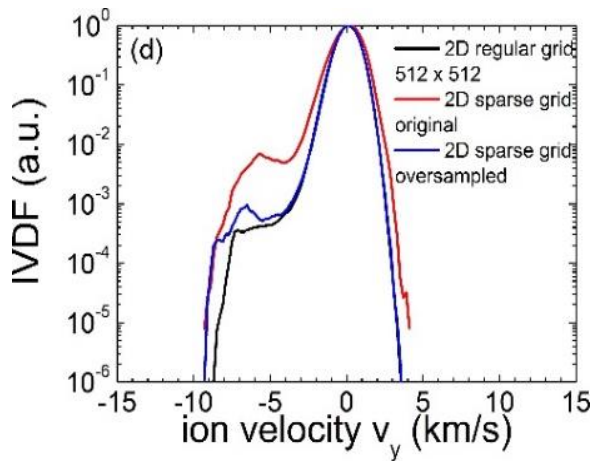
**Regular 512 x 512**  
**Npc: 400**



**Sparse N = 9**  
**Npc: 400**  
**Gain in comp. time: 6.5**

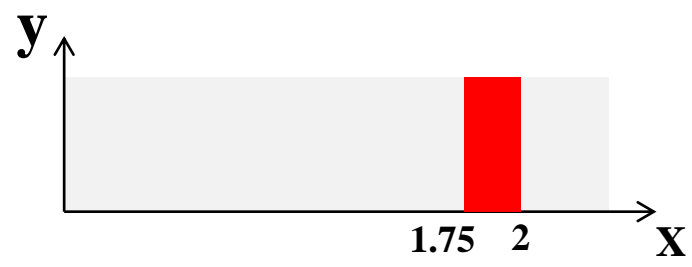


**Sparse N = 9, offset**  
**Npc: 400**  
**Gain in comp. time: 4**

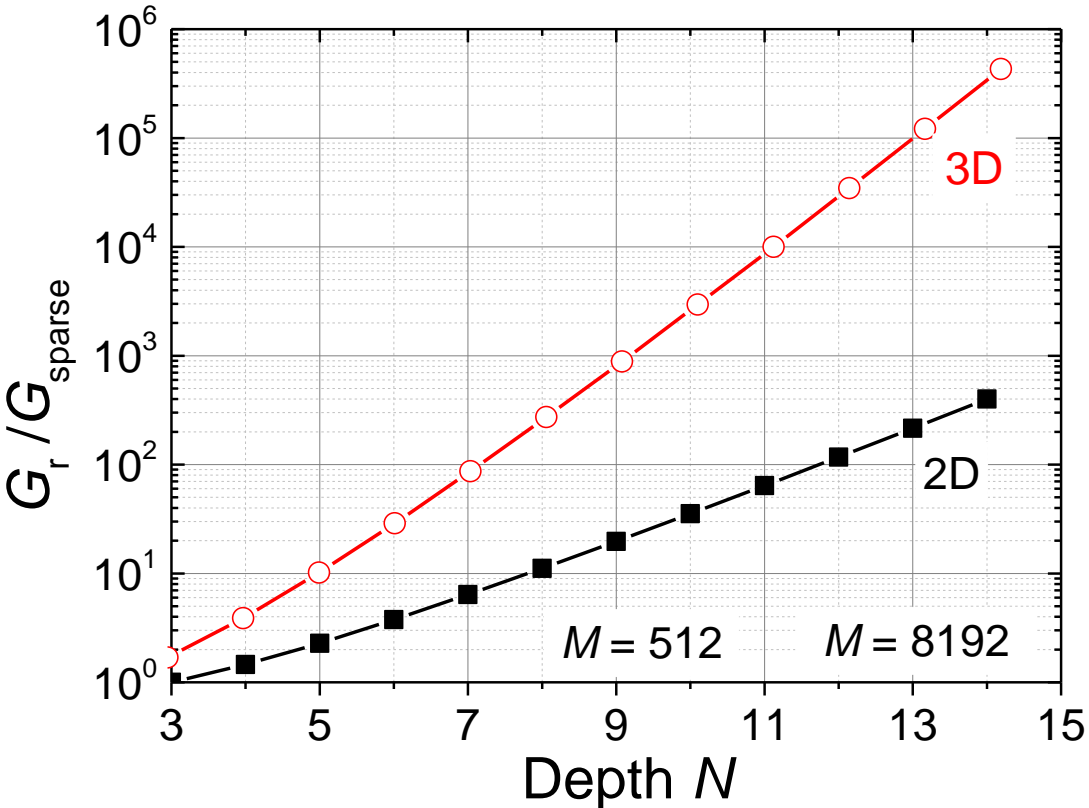


*L. Garrigues et al., J. Appl. Phys.*  
*129, 153304 (2021)*

*L. Garrigues et al.,*  
*ESCAMPIG (2022)*



# Number of cells in 3D



**large speed up expected for 3D simulations**

# Conclusions

- **Applicability of PIC simulations to model plasma thrusters**
  - More studies with the electrostatic approximation (Hall Thruster, GIE)
  - Electromagnetic PIC algorithms more difficult to implement
  - Very time consuming
- **PIC schemes take advantages of efficient parallelization techniques** (OpenMP-MPI hybrid parallelization)
- **Acceleration of PIC schemes**
  - Sparse approach seems promising (cusp magnetic field can be included)
  - Others approaches exist (implicit version, reduced dimensional order method, etc.)

# Open questions/Perspectives

- A full coupling between Maxwell's equations and the plasma is difficult to achieve but a self-consistent calculation of power absorption is reachable
- Heterogeneous architecture of computers (GPU/CPU)
- Plasma-wall interactions and necessary data
- Elementary data - cross sections for new propellant gases (iodine)

# For more details

- To appear in Journal of Applied Physics
- <https://arxiv.org/abs/2304.05103>

Plasma propulsion simulation using particles

## Plasma propulsion simulation using particles

F. Taccogna,<sup>1</sup> F. Cichocki,<sup>1</sup> D. Eremin,<sup>2</sup> G. Fubiani,<sup>3</sup> and L. Garrigues<sup>3</sup>

<sup>1</sup>*Institute for Plasma Science and Technology (ISTP), CNR, Bari, Italy*

<sup>2</sup>*Institute of Theoretical Electrical Engineering, Ruhr University Bochum, Universitätsstraße 150, 44801 Bochum, Germany*

<sup>3</sup>*LAPLACE, Université de Toulouse, CNRS, INPT, UPS, Toulouse, France*

(\*Electronic mail: francesco.taccogna@cnr.it)

(Dated: 29 September 2023)

This perspective paper deals with an overview of particle-in-cell / Monte Carlo collision models applied to different plasma-propulsion configurations and scenarios, from electrostatic ( $\mathbf{E} \times \mathbf{B}$  and pulsed arc) devices to electromagnetic (RF inductive, helicon, electron cyclotron resonance) thrusters, with an emphasis on plasma plumes and their interaction with the satellite. The most important elements related to the modeling of plasma-wall interaction are also presented. Finally, the paper reports new progress in the particle-in-cell computational methodology, in particular regarding accelerating computational techniques for multi-dimensional simulations and plasma chemistry Monte Carlo modules for molecular and alternative propellants.

# Acknowledgments

- **Sparse PIC Project: Fundings from ANR-22-CE46-0012 under the MATURATION project**



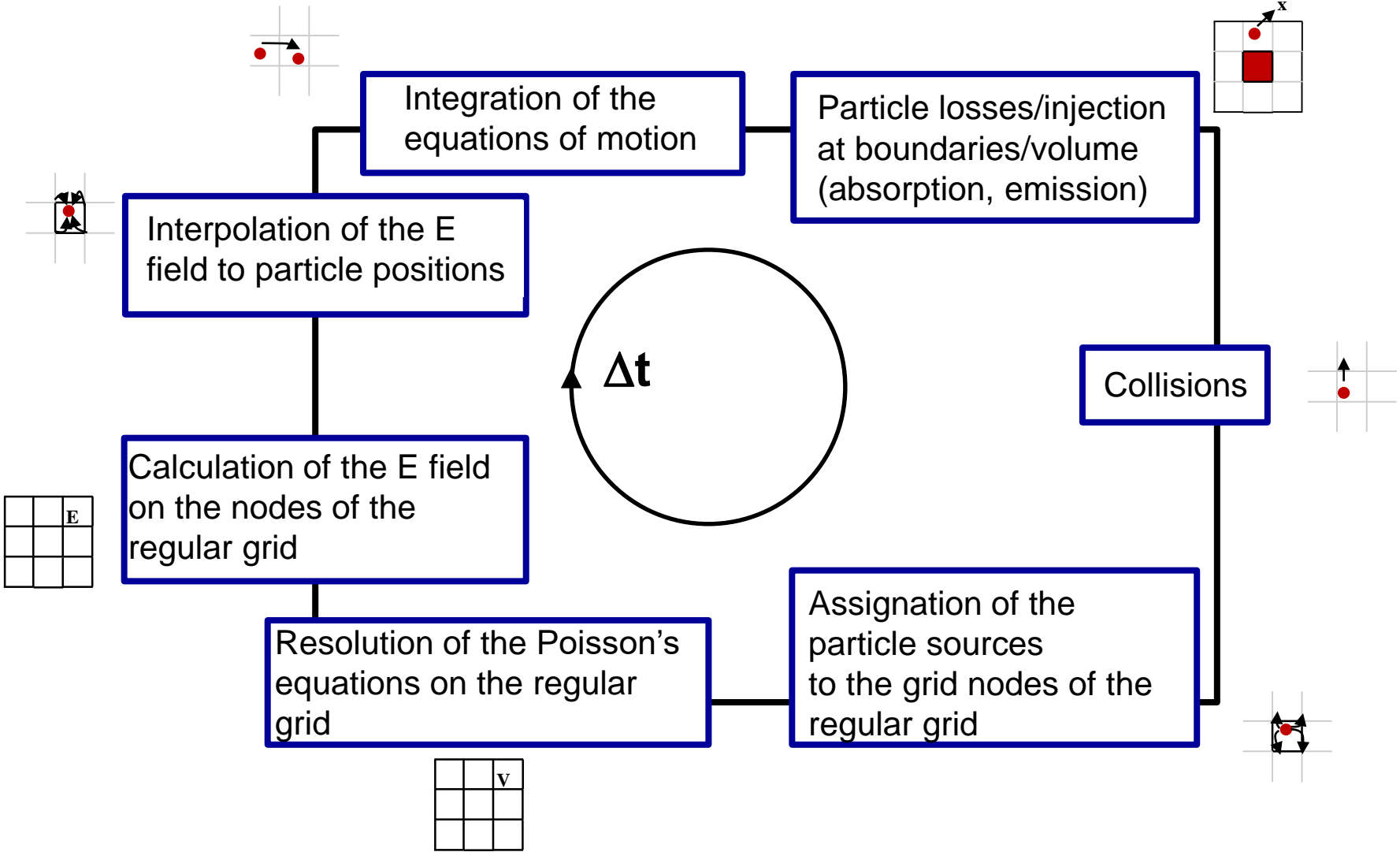
- **Super calculator CALMIP/Olympe (Toulouse University)**



# Additional slides



# PIC cycle with the electrostatic approach

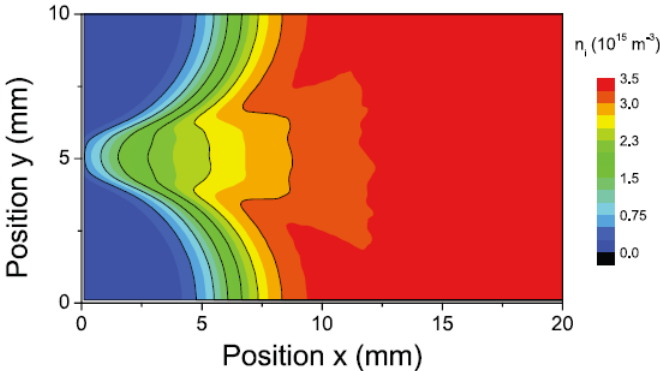
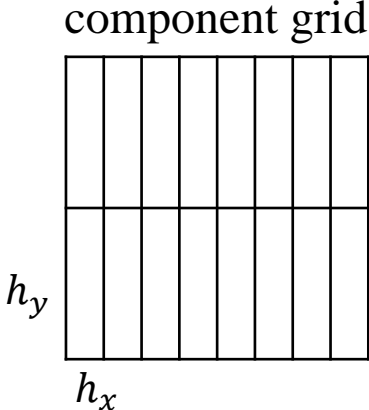


# More about the grid-based error

- Grid-based error in 2D**

- Terms along  $x$  and  $y$  directions cancel out with combination technique ... but not along mixed directions
- Error associated with  $\rho$

$$\epsilon_s = \underbrace{b_1 \frac{\partial^2 \rho}{\partial x^2} h_x^2}_{\text{error along } x} + \underbrace{b_2 \frac{\partial^2 \rho}{\partial y^2} h_y^2}_{\text{error along } y} + \underbrace{b_{1,2} \frac{\partial^4 \rho}{\partial x^2 \partial y^2} h_x^2 h_y^2}_{\text{error along mixed directions}} + O(h_x^4, h_y^4)$$



Y. Jiang *et al.*, *Phys. Plasmas* 27, 113506 (2020)

Contents lists available at [ScienceDirect](https://www.sciencedirect.com)

**Journal of Computational Physics**

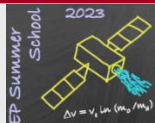
journal homepage: [www.elsevier.com/locate/jcp](http://www.elsevier.com/locate/jcp)

Efficient parallelization for 3d-3v sparse grid Particle-In-Cell: Shared memory architectures

Fabrice Deluzet<sup>a</sup>, Gwenael Fubiani<sup>b</sup>, Laurent Garrigues<sup>b</sup>, Clément Guillet<sup>a,b,\*</sup>, Jacek Narski<sup>c</sup>

- Oversampled method to reduce the grid-based error in the mixed directions**

S. Muralikrishnan *et al.*, *J. Comput. Phys. X* 11, 100094 (2021)

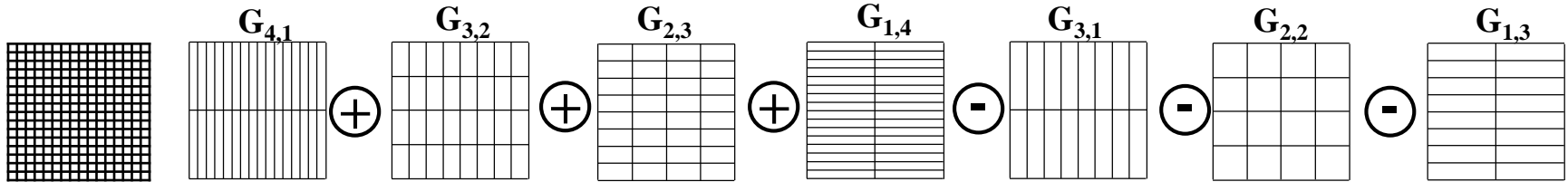


# The offset sparse method – component grids

$$l^0 = 0, l^1 = 0 \text{ and } k, m \geq 1$$

$$k + m = n + l^0 - l^1 + 1 = 5$$

$$k + m = n + l^0 - l^1 = 4$$



$$16 \times 16$$

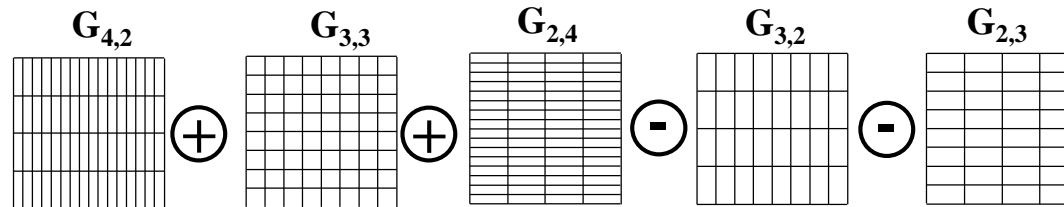
$$2^I \times 2^J$$

$$I = J = n = 4$$

$$l^0 = 1, l^1 = 0 \text{ and } k, m > l^0$$

$$k + m = n + l^0 - l^1 + 1 = 6$$

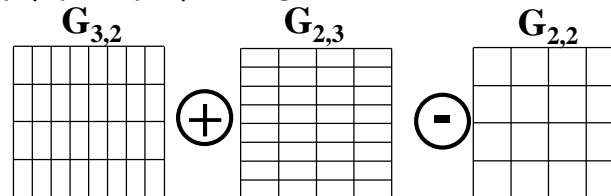
$$k + m = n + l^0 - l^1 = 5$$



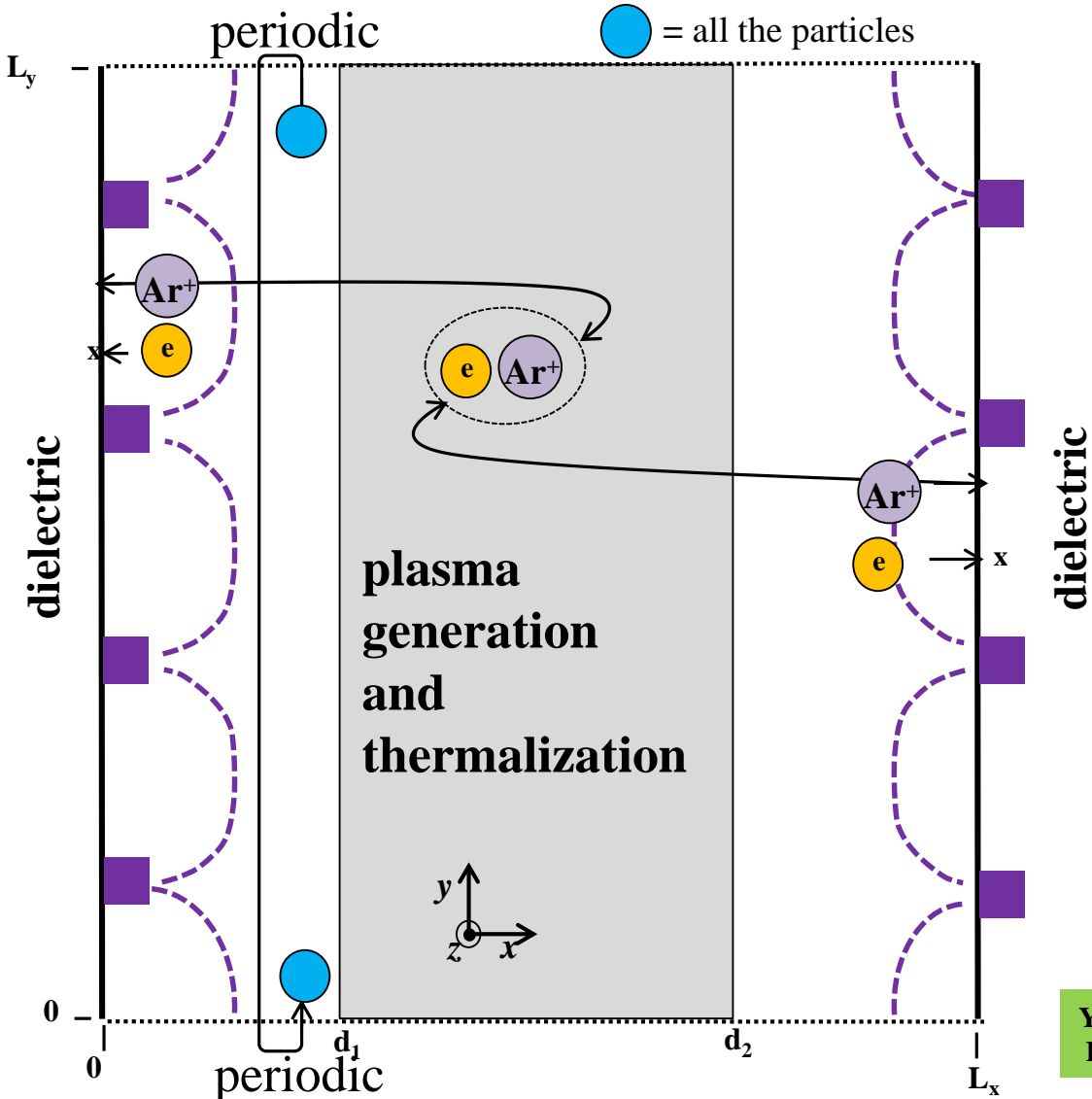
$$l^0 = 1, l^1 = 1 \text{ and } k, m > l^0$$

$$k + m = n + l^0 - l^1 + 1 = 5$$

$$k + m = n + l^0 - l^1 = 4$$



# Simplified 2D modeling of a cusp discharge



*Discharge characteristics*

- Magnetized electrons, argon ions
- Initial electron temperature (eV) 3
- Thermalization temperature (eV) 3
- Initial ion temperature (eV) 0.1
- Electron-neutral collisions

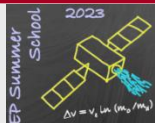
*Initial conditions*

- Pressure (mTorr) 0.1
- Neutral density ( $10^{18} \text{ m}^{-3}$ ) 3.2
- Initial plasma density ( $10^{15} \text{ m}^{-3}$ ) 1
- Magnetic field max (G) 400

*Simulation conditions*

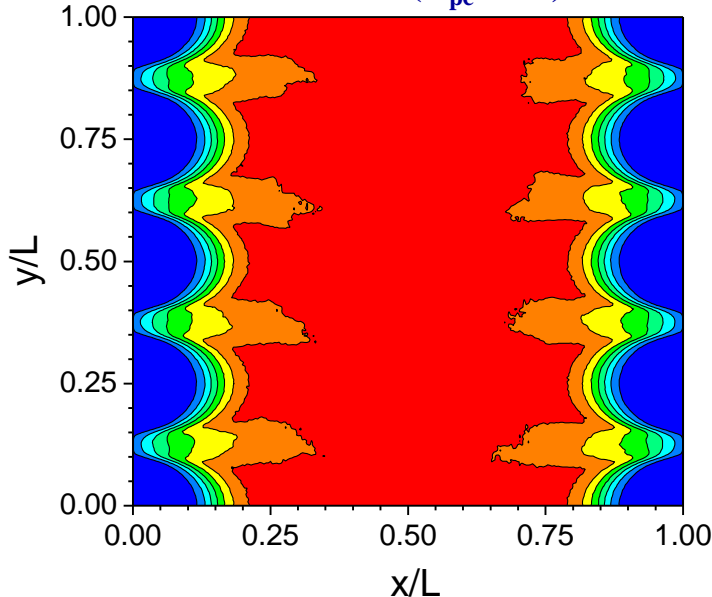
- $L_x = L_y$  (cm) 4
- $d_1, d_2$  (cm) 1.6, 2.4
- Number of grid cells (std)  $256^2$
- Time step ( $\text{s}^{-1}$ )  $0.2/\omega_p$
- $N_{PC}$  50

Y. Jiang, G. Fubiani, L. Garrigues, and J. P. Boeuf, Phys. Plasmas 27, 113506 (2020)

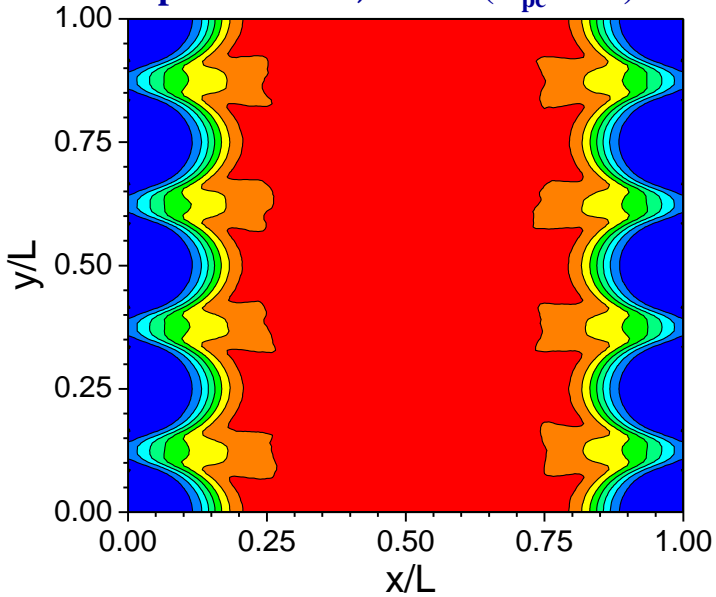


# Results @ 0.1 mTorr - 400 G

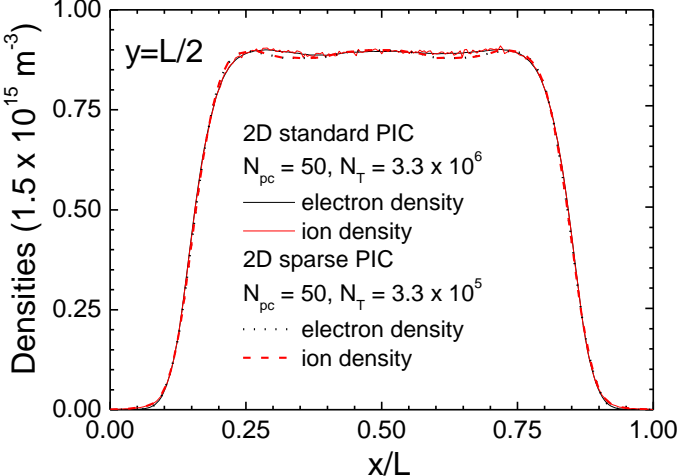
Standard ( $N_{pc} = 50$ )



Sparse  $l^0 = 4, l^1 = 1$  ( $N_{pc} = 50$ )



Ion density  
 $1.4 \times 10^{15} \text{ m}^{-3}$



$$\epsilon(\varphi) = \frac{\|\varphi - \varphi_{\text{ref}}\|_{L^2}}{\|\varphi_{\text{ref}}\|_{L^2}} = \sqrt{\frac{\int |\varphi - \varphi_{\text{ref}}|^2 du}{\int |\varphi_{\text{ref}}|^2 du}}$$

Error (%)	
$n_i$ (2D)	4.5
$n_e$ (2D)	4.5

L. Garrigues et al.,  
in preparation

